

1                    **Illuminating the transition from an open to a**  
2                    **semi-closed volcanic vent system through episodic**  
3                    **tremor duration and shape**

4                    **Eva P. S. Eibl<sup>1</sup>, Thor Thordarson<sup>2</sup>, William M. Moreland<sup>2</sup>, Egill Árni**  
5                    **Gudnason<sup>3</sup>, Ármann Höskuldsson<sup>2</sup>, Gylfi Páll Hersir<sup>4</sup>**

6                    <sup>1</sup>University of Potsdam, Institute for Geosciences, Karl-Liebknecht-Str. 24/25, Potsdam-Golm, Germany  
7                    <sup>2</sup>University of Iceland, Sturlugata, Reykjavík, Iceland  
8                    <sup>3</sup>ISOR, Iceland GeoSurvey, Urdarhvarf 8, Kópavogur, Iceland  
9                    <sup>4</sup>Independent Researcher, Reykjavík, Iceland

10                    **Key Points:**

- 11                    • The 2021 Geldingadalir eruption in the Fagradalsfjall Fires, Iceland, featured 8696  
12                    tremor episodes of minute to week duration.
- 13                    • An open vent system with lava residing in the crater during repose featured minute-  
14                    long lava effusion with bell- or rectangle-shaped tremor.
- 15                    • A semi-closed vent system with no lava residing in the crater featured hour-long  
16                    lava effusion with ramp-shaped tremor.

---

Corresponding author: Eva P. S. Eibl, [eva.eibl@uni-potsdam.de](mailto:eva.eibl@uni-potsdam.de)

## Abstract

[Volcanic eruptions generate continuous or episodic tremor, which can provide unique information about activity changes during eruption. However, the wealth of information in episodic tremor patterns is often not harvested and transitions between patterns remain obscure. The 2021 Geldingadalir eruption of the Fagradalsfjall Fires, Iceland, is an exceptional case, where the lava effusion caused continuous tremor, and 8696 tremor episodes spanning two orders of magnitude in duration and repose. Based on seismometer and video camera data, we associate several-minute-long, symmetrical episodes with an open vent system, where lava remains in the crater bowl during repose, connected to a shallow magma compartment. Ramp-shaped episodes, lasting several hours, are associated with a temporary closure of the vent system, where no lava remains in the crater bowl during repose and more time is required to resume effusion. The transition from continuous to episodic effusion is related to the cumulative time spent in effusion and repose, and to external factors like crater wall collapses.]

## Plain Language Summary

Volcanic eruptions can provide unique information about the subsurface structure and processes driving it. Often effusion happens continuous over a time span. However, sometimes the effusion starts and stops and is hence episodic. During the 2021 Geldingadalir eruption, Iceland the lava flowed continuously from the vent but later stopped 8696 times. Some of these episodes were a few minutes long, while others lasted several hours. We interpret several-minute-long episodes as an open system, where lava remains in the crater during repose. This system can restart fast and easy. During several hour-long episodes, no lava remains in the crater during repose. The system needs more time to reopen the vent. The system also reacts depending on the time it is in repose or effusion. And finally, external factors like crater wall collapses modify the episodic pattern.

## 1 Introduction

Volcanic tremor is an emergent, long-lasting seismic ground motion that does not have clear seismic phases that arrive at specific times like earthquakes. It has been identified as a crucial tool for monitoring volcanic processes both at depth and as they emerge at the surface during a volcanic eruption (McNutt, 1996; McNutt et al., 2015). Deep tremor can be associated with magma storage areas or pathways (Battaglia et al., 2005a; Patane et al., 2008; E. P. Eibl, Bean, Vogfjörð, et al., 2017; Li et al., 2022; Journeau et al., 2022). Near the surface, it accompanies volcanic eruptions and can be used to understand the processes that generate tremor. Some studies relate it to the cross-sectional area of the vent (McNutt & Nishimura, 2008), the effusion rate (Koyanagi et al., 1987; Battaglia et al., 2005b; Falsaperla et al., 2005; Coppola et al., 2009) or the fountain height (Alparone et al., 2003; McNutt, 1987; Koyanagi et al., 1987), while others find no correlation with effusion rate (E. P. Eibl, Bean, Jónsdóttir, et al., 2017; Coppola et al., 2009; Allard et al., 2011) or fountain height (Aki & Koyanagi, 1981; Eaton et al., 1987; E. P. S. Eibl et al., 2023). Tremor monitoring and observations are particularly important for tracking eruption progress in remote areas or during periods of low visibility (Yukutake et al., 2017; E. P. S. Eibl et al., 2023; Langer et al., 2009).

However, tremor research faces several challenges. For example, tremor is often characterised by gradual onsets, where the signal emerges from the noise (Konstantinou & Schlindwein, 2003). This tremor is more difficult to detect and assess than the few cases that feature impulsive onsets (Aki & Koyanagi, 1981; Fehler, 1983). However, it is important to determine the onset accurately, as for example Alparone et al. (2003) showed during 64 lava fountaining events at Mount Etna, Italy in 2000 that the time taken to rise from the start to the maximum tremor amplitude was strongly related to the total

duration of the tremor episode. They used this relationship to estimate the end times of the tremor and the associated volcanic activity.

Tremor can persist continuously for months or years. More importantly, the underlying processes can also generate episodic tremor (Moschella et al., 2018; Alparone et al., 2003; Michon et al., 2007; E. P. S. Eibl et al., 2023). In such cases, the duration of tremor episodes or repose periods are often not assessed in detail. Notable exceptions are the studies by E. P. S. Eibl et al. (2023); Alparone et al. (2003); Moschella et al. (2018); Michon et al. (2007); Andronico et al. (2021), which assess episodic tremor whose changes in duration and repose time are less than an order of magnitude. Increases or decreases in duration of at least one order of magnitude within an episodic pattern are rarely observed, appear as outliers and their origin is unfortunately not further discussed in these publications (Privitera et al., 2003; Heliker & Mattox, 2003; Spampinato et al., 2015; Calvari et al., 2011; Alparone et al., 2003). Most of these studies only report the duration without providing an interpretation of the trends observed. E. P. S. Eibl et al. (2023) have taken this last step and interpreted the gradual and sudden changes in episode duration as a sign of a shallow magma compartment that first developed for 11 days after the onset of episodic activity and then stabilised. They interpreted the repose time in the context of the amount of degassed material accumulating in the crater edifice.

Finally, few studies have evaluated the shape of the tremor (Alparone et al., 2003; McNutt & Nishimura, 2008; Viccaro et al., 2014). McNutt and Nishimura (2008) studied 24 eruptions at 18 volcanoes and described three typical stages of eruption tremor: an exponential increase, a sustained or fluctuating maximum tremor amplitude, and an exponential decrease. These increases and decreases can last from minutes to hours, and while they assessed how many eruptions featured an exponential increase or decrease, they did not discuss the underlying reasons for the shape. Alparone et al. (2003); Viccaro et al. (2014) classified tremor episodes on Mt. Etna as ramp shape (slow amplitude increase and rapid decrease), bell shape (amplitude increase and decrease at similar rates) and tower shape (sudden amplitude increase and decrease). These types may feature the same decrease rates but different increase rates, and again a thorough interpretation of these shapes in the context of the volcanic behaviour is lacking.

To use tremor effectively, we need to understand the details of tremor, which is often limited by poor instrumentation, a lack of high-quality multidisciplinary data, and a lack of detail in the tremor studies.

Here, we provide an overview of 8696 tremor episodes of the Geldingadalir eruption from May to September 2021 (section 2) recorded using a seismic network. We present changes in the effusion pattern and the crater edifice (section 4.1), sudden increases of two orders of magnitude in tremor duration and repose time that are maintained for months (section 4.2 and 4.3), and a systematic change in the tremor amplitude increase rates (section 4.4). We discuss trends in the several minute-long episodes (section 5.1), the order of magnitude increases in repose time and episode duration (section 5.2), the transition from minute-long to hour-long to day-long episodes to continuous tremor (section 5.3), and the evolution of the tremor shape with time (section 5.4).

## 2 Overview of the 2021 Geldingadalir eruption site

The Reykjanes Peninsula, SW Iceland, is the onshore continuation of the Mid-Atlantic Ridge. The divergent plate boundary of the North American and Eurasian plates comes ashore at the SW tip of the peninsula, and extends from there as a 60 km long N70°E striking oblique rift (Sigmundsson et al., 2020). The oblique rift, or trans-tensional zone, is expressed by a 5-10 km wide seismic and volcanic zone. It is highly oblique with a spreading direction of N120°E in this region compared to the global plate motion in Iceland which spreads at a rate of 18-19 mm/yr in the direction of N105°E (Keiding et al., 2009; Sigmundsson et al., 2020; Sæmundsson et al., 2020). The divergence of the plates is expressed in five rift segments, arranged en-echelon on the peninsula, which accommodate the rifting (Sæmundsson et al., 2020). These rift segments, or volcanic systems, are ar-

120 eas with the highest density of eruptive fissures and tectonic fractures and faults. They  
 121 are, from west to east: Reykjanes, Eldvörp-Svartsengi, Fagradalsfjall, Krýsuvík and Bren-  
 122 nisteinsfjöll (Fig. 1a).

123 The detailed eruptive record of volcanic activity on the Reykjanes Peninsula over  
 124 the last 4000 years shows a periodic pattern, where 300 to 500 year long periods of rift-  
 125 ing and volcanism are separated by 800 to 1000 year long periods of volcanic quiescence  
 126 (Sæmundsson et al., 2020). Also, within each eruptive period, the whole of the Reyk-  
 127 janes Peninsula, from Brennisteinsfjöll in the east to Reykjanes in the west, seems to be  
 128 activated, with the last eruptive period culminating 781 years ago (Jónsson, 1983; Sæ-  
 129 mundsson et al., 2020; Sigurgeirsson, 1995). However, the last eruptive activity in the  
 130 Fagradalsfjall volcanic system occurred more than 6000 years ago (Sæmundsson & Sig-  
 131 urgeirsson, 2013). The Fagradalsfjall Fires may signal the beginning of a new eruptive  
 132 period on the Reykjanes Peninsula.

133 The 2021 Geldingadalir eruption began at 20:40 UTC on 19 March 2021 (Sigmundsson  
 134 et al., 2022) within the Fagradalsfjall volcanic system on the Reykjanes Peninsula. It was  
 135 preceded by several seismic swarms on the peninsula from 2019 to 2021 and intrusions  
 136 in 2020 (Çubuk-Sabuncu et al., 2021; Flóvenz et al., 2022; Geirsson et al., 2021). The  
 137 last swarm before the eruption started on 24 February 2021 and, interestingly, the de-  
 138 formation and seismicity decreased for several days before the eruption started (Fischer  
 139 et al., 2022; Sigmundsson et al., 2022). This last swarm was partly associated with the  
 140 formation/emplacement of a 9 km long dike (Sigmundsson et al., 2022). The eruption  
 141 started at its southern end in a zone of extension (Fischer et al., 2022).

142 From the start of the eruption on 19 March until 5 April, only one vent system was  
 143 active featuring continuous lava effusion (Fig. 1). From 5 to 13 April more vents opened  
 144 (Vent-2 to Vent-6) and by 27 April the only active vent was Vent-5 (E. P. S. Eibl et al.,  
 145 2023; Pedersen et al., 2022). Vent-5 had developed a sustained low-intensity lava foun-  
 146 taining on 25 April and changed to a minute-scale episodic behaviour on 2 May (E. P. S. Eibl  
 147 et al., 2023). It has been suggested that this may be related to a change in magma com-  
 148 position from depleted to enriched olivine tholeiite in conjunction with a doubling of the  
 149 magma discharge rate in late April (Pedersen et al., 2022; Thordarson et al., 2023) and  
 150 changes in the shallow subsurface (E. P. S. Eibl et al., 2023). These minute-long lava foun-  
 151 tain episodes continued until 13 June (E. P. S. Eibl et al., 2023). Here we highlight the  
 152 orders of magnitude increase in episode duration and repose time from the minute scale  
 153 in May to June, the hour scale from July to early September, and the day scale in Septem-  
 154 ber.

155 The eruption ended on 18 September. The average effusion rate (assuming 1/3 void  
 156 space) from March to mid-April was  $4 \text{ m}^3/\text{s}$  and increased to  $8 \text{ m}^3/\text{s}$  from May (Pedersen  
 157 et al., 2022; Thordarson et al., 2023). The eruption had covered a  $4.8 \text{ km}^2$  large area at  
 158 a bulk volume of  $0.15 \text{ km}^3$  (Pedersen et al., 2022), where the dense rock equivalent (DRE)  
 159 value is  $\sim 0.11 \text{ km}^3$  (Thordarson et al., 2023).

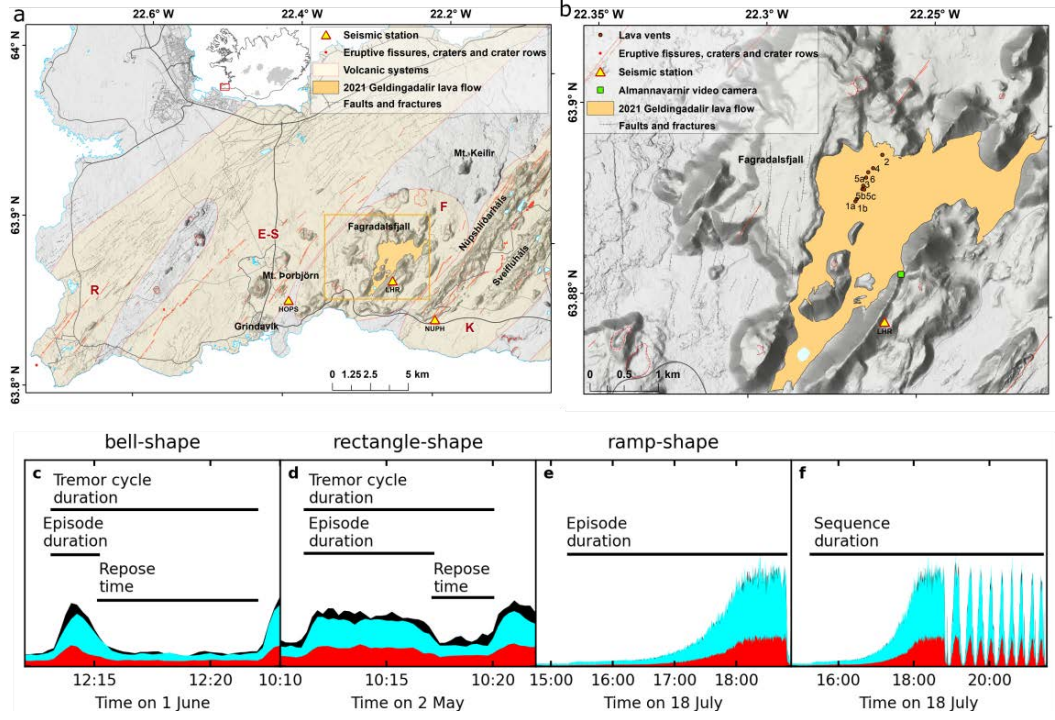


**Figure 1.** Seismic network near the 2021 Geldingadalir eruption site. (a) Four of the five volcanic systems on the Reykjanes Peninsula (light brown) from west to east: Reykjanes (R), Eldvörp-Svartsengi (E-S), Fagradalsfjall (F), Krýsuvík (K) (Sæmundsson & Sigurgeirsson, 2013). We show the lava flow field in beige and the seismometers with triangles. The inset marks the location in Iceland. (b) Extent of the lava flow field on 18 September 2021 as derived by the National Land Survey of Iceland, the University of Iceland and the Icelandic Institute of Natural History (Bindeman et al., 2022; Halldórsson et al., 2022). (c-e) Examples of (c) bell-shaped, (d) rectangle-shaped and (e) ramp-shaped tremor. (c-f) Definition of tremor cycle duration, episode duration, repose time and a tremor sequence.

### 3 Material and Methods

#### 3.1 Instrument Network

To monitor the seismic signals caused by the 2021 Geldingadalir eruption, we installed a Trillium Compact 120 s seismometer 5.5 km southeast of the eruption site in the lowland just east of Núpshlíðarháls (station NUPH in Fig. 1a, 9F seismic network) (E. P. S. Eibl, Hersir, et al., 2022). This station was installed on 12 March 2021 and dismantled on 24 June 2021 due to wind noise, oceanic microseism and surf noise. We installed the seismometer on the same day east of Langihryggur at 1.8 km distance from the eruptive vent (station LHR, 9F seismic network) (Fig. 1b). We also use data from a seismometer at HOPS, located near Grindavík 7 km southwest of the active vent. It recorded from 24 July 2021.

At all sites, we used a concrete base plate and a compass to align the sensor to geographic north. While the seismometers at NUPH and HOPS were protected from the wind by a bucket and rocks, the seismometer at LHR was dug about 90 cm deep into the ground. At NUPH and HOPS it was powered using batteries, solar panels and a wind generator, while at LHR we had access to permanent power from a generator at 1.5 km distance near the main road. Ground motion was sampled at 200 Hz at all sites, with the data stored on a Datacube and downloaded regularly. The data quality is good enough to assess the volcanic tremor generated throughout the whole 2021 Geldingadalir eruption. There are small gaps in the time series on 24 June from 10:30 to 15:16 UTC due to field work and from 14:00 on 2 July to 9:26 on 6 July due to a power outage. The episodic tremor pattern in the gap in July can be assessed using station HOPS.

#### 3.2 Automatic Picking of Tremor Episodes

To mark the start and end of the tremor episodes we use a STA/LTA triggering algorithm (Trnkoczy, 2012) as implemented in the Pyrocko trace-viewer Snuffler (Heimann et al., 2017). We apply the STA/LTA trigger to the sum of 3-component seismic data from station NUPH and LHR, filtered with a 0.5 to 4 Hz Butterworth filter. We choose a short window (STA) of 60 to 120 s and a long window (LTA) of 180 to 360 s. This approach generates markers automatically and we check them manually and adjust them with the onset of the tremor episode if necessary. We repeat this procedure to generate markers at the end of the episodes.

To mark hour-long episodes we use the root mean square (RMS) tool as implemented in Snuffler. This allows us to assess the RMS amplitude on longer timescales and to manually place a marker at the start of these tremor episodes (Fig. 1c-f). We delete 196 markers (=98 episodes) in the catalog of E. P. S. Eibl, Roskopf, et al. (2022) after 16:00 on 13 June 2021, as they were re-identified as pulses, because the tremor does not completely stop during the lull between subsequent tremor peaks. This change does not affect the conclusions presented in (E. P. S. Eibl et al., 2023). In summary, our final catalog contains 17392 markers indicating the start and end of 8696 episodes between 2 May and 18 September 2021. 6959 episodes occurred before 14 June and 1737 episodes after 14 June.

We use our markers to calculate the **episode duration** and **repose time**, which in sum yield the **episode cycle duration** (Table 1 and Fig. 1c). We create an additional marker list to assess the **sequence duration** comprised of an hour-long episode and several minute-long episodes (Table 1 and Fig. 1f).

#### 3.3 RMS Calculation

We also assess the seismic amplitude and therefore detrend, taper and instrument correct the data. We then apply a Butterworth bandpass filter of order 4 to filter the data (unit: velocity) from 0.5 to 4 Hz. We use Obspy (Beyreuther et al., 2010) to cal-



209 culate the RMS in 30 s long moving time windows with 50% overlap. Additionally, we  
 210 calculated the mean RMS in time windows from the start to the end of a tremor episode.

211 For illustrative purposes only, we fill the data gap from 14:00 on 2 July to 9:26 on  
 212 6 July at LHR with RMS amplitudes from HOPS. We compare the RMS amplitudes at  
 213 HOPS and LHR from 17:07:13.875 to 17:14:43.875 on 6 July to assess whether the dif-  
 214 ference in tremor amplitude is due to the difference in distance from the eruption site.  
 215 To adjust for the difference in tremor amplitude, we multiply the HOPS RMS amplitude  
 216 by 7.8 before plotting (Fig. 2c and d).

217 We repeat this procedure for the RMS amplitude of NUPH and HOPS in the time  
 218 window from 10:09:15 to 10:21:45 on 24 June 2021. We multiply the amplitude of NUPH  
 219 with 10.9 which is the average of the ratio for all three components (Fig. 2c and d).

### 220 3.4 Drone data analysis

221 The 3D vent models of 11 July were created using photogrammetry in Pix4D Map-  
 222 per. The photographs used for this were collected during two grid flights flown with a  
 223 DJI Matrice 300 RTK quadcopter using an H20T camera module. A total of 488 pho-  
 224 tographs were taken in a grid layout around the vent with oblique and nadir orientations.  
 225 The primary products of the Pix4D Mapper were Wavefront OBJ 3D models. These mod-  
 226 els were imported into Maptek PointStudio where the internal volume of the vent was  
 227 measured using a horizontal plane level with the lowest point of the vent ramparts as  
 228 the uppermost surface.

229 We estimate the minimum volume of a block that broke off on 11 July. We were  
 230 conservative in placing the bounding edges of the block. The dimensions of the block that  
 231 formed on 11 July were estimated by analysing a photogrammetric 3D model from a time  
 232 before block formed. The 3D model was imported into Maptek PointStudio, where the  
 233 edges of the block were delineated based on cracks which were observed from UAS sur-  
 234 veys and from observations of the extent of the block visible on web cameras operated  
 235 by the Department of Civil Protection and Emergency Management (Almannavarnir).  
 236 The basal surface of the block was determined from the elevation of the break in slope  
 237 between the vent ramparts and the surrounding lava.

### 238 3.5 Video Camera Data Analysis

239 Similarly to E. P. S. Eibl et al. (2023), we used the camera from Almannavarnir  
 240 on Langihryggur hill, at 1.3 km distance from Vent-5, for our processing. We assess the  
 241 vent height and shape as seen from the southeast (Fig. 1b). To do this, we extract frames  
 242 from the video using a VLC media player and map the shape of the crater using Inkscape.  
 243 The frames were aligned using the shape of mount Fagradalsfjall in the background. The  
 244 scale is derived from people and cars near the vent at the start of the eruption, and we  
 245 estimate an uncertainty in height of  $\pm 2$  m.

## 246 4 Results

### 247 4.1 Lava Pond and Partial Collapses of Crater-5

248 During May and until mid-June, outgassed lava remained in the Crater-5 during  
 249 repose. During the tremor episodes, the lava filled the crater bowl to the level of the low-  
 250 est breach in the crater edifice, producing the surface outflow from the crater and lava  
 251 fountains (Fig. 2a). For most of May, this breach was at relatively low elevation com-  
 252 pared to the bulk of the crater ramparts - about 10 m above the surrounding lava, com-  
 253 pared to 40 to 50 m for the highest part of the crater (E. P. S. Eibl et al., 2023). Around  
 254 27 to 28 May the level of the breach began to rise and by 30 to 31 May it had reached  
 255 a level similar to the rest of the crater. From then on until 14 June, the crater bowl was  
 256 filled with lava to the rim during a tremor episode. Some of the residing lava in the crater

bowl, was pushed out at 4:10:18 on 10 June during a major collapse of an overhanging roof into the crater. This reduced the duration of repose and the tremor amplitude of the subsequent episodes, as described in E. P. S. Eibl et al. (2023).

Following continuous tremor for most of June, it stopped rapidly at 0:57 on 2 July and no lava was present in the crater edifice during the morning and afternoon of 2 July during repose. On 2 July, between 3:00 and 5:00, a series of eight unusual and very dark, gas charged, and possibly dust-rich plumes rose from Crater-5. The size and longevity of these plumes suggest major changes to the upper part of the conduit system, such as widening/enlargement of the top of the shallow conduit and the crater bowl. There are no changes to the outer visible parts of the crater. Due to poor visibility and a growing edifice, we cannot assess when it first emptied completely during repose or when this became a common occurrence between episodes.

From 11 to 16 July, major changes on the crater edifice happened. At 22:59:48 on 10 July a small part of the NE rim collapsed. At 3:48 on 11 July, no cracks are visible on the NE crater wall in our drone footage. However, between 4:22 and 9:00 a large part of the NE crater rim broke off, forming a breach in the crater (Fig. 3). This flank is lower and less thick and therefore more prone to collapse than the southern flank. We estimate a volume of about  $2 \cdot 10^5 m^3$  and assuming a density of  $1500 kg/m^3$  the approximate mass is  $3 \cdot 10^8 kg$ . Until the evening of 16 July, a detached block remained in the crater area, moving up and down during episodic lava effusion. By 17 July the crater wall had increased in height and thickness and the detached block stopped moving. Our records show that on 20 July lava remained in the crater edifice during repose, whereas from 26 July until the end of the eruption no lava remained during repose (Fig. 2b).

In early September, Vent-5 became blocked, resulting in a 1-week-long repose time. On 11 September the magma found a new way to the surface at the foot of the wall of Crater-5. This outlet is located a few tens of meters northwest of the former Vent-5 and spilled lava back into the old crater and to the outside of the crater rim onto the old lava flow field (Fig. 3). The crater reached a final height of 110 m above the pre-eruptive surface (Pedersen et al., 2022).

## 4.2 Short Episodes and Continuous Tremor

The observed seismic tremor episodes (Table 1) are in phase with the fountaining episodes that typified the activity at Vent-5 for most of its lifetime (see E. P. S. Eibl et al. (2023); Lamb et al. (2022) for examples in May). However, the initial increase in tremor preceded any visible lava outflow from the crater and instead accompanied the magma as it emerged from the vent and slowly filled the crater. Based on the number of tremor episodes per time unit, we divide the eruption into 6 phases. (I) Continuous lava effusion from one or more vents, (II) episodic tremor on minute-scale from Vent-5, (III) continuous tremor followed by both minute and hour-long episodic tremor, (IV) sequences of one ramp-shaped tremor and several minute-long bell-shaped episodic tremor, (V) several ramp-shaped, hour-long episodic tremor and (VI) one ramp-shaped tremor followed by several minute-long episodes (Fig. 2b).

The episodes are detected on all 3 components of the seismometer throughout the whole eruption. There are no major changes in the wavefield (Fig. 2c). Filtered from 0.5 to 4 Hz, the mean seismic amplitude is 3 to  $5 \cdot 10^{-6} m/s$  during most episodes. Larger amplitudes are reached only during minute-long episodes in July and September. The largest overall tremor amplitudes reach mean amplitudes of up to  $9 \cdot 10^{-6} m/s$  in July (Fig. 2d and 4a).

The activity in **Phase II** from 2 May to 10:00 on 13 June 2021 was dominated by several minute-long episodes and repose times, with both gradual trends and sudden increases or decreases. This could be correlated with certain changes in the vent conditions (geometry and state of the magma) and the crater edifice as further detailed in E. P. S. Eibl et al. (2023). The continuous tremor resumed on 13 June (Fig. 2c).



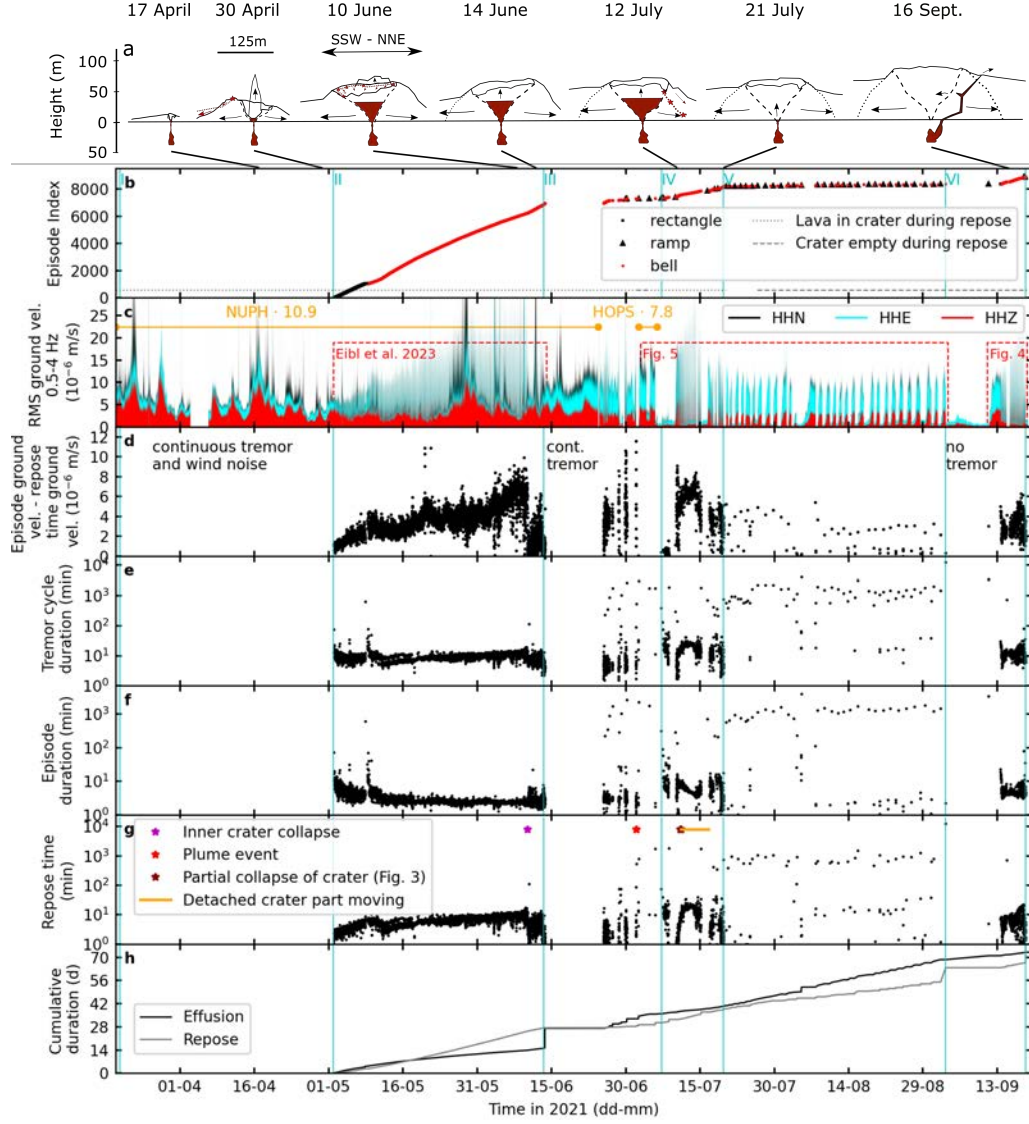


**Figure 2.** Transitions between continuous and episodic tremor from 19 March to 18 September 2021. (a) Evolution of Crater-5 growth. (b) Evolution of the episodic tremor pattern over time. The marker type indicates the tremor shape as rectangle (black dot), ramp (black triangle) or bell (red dot). Dotted and dashed horizontal lines mark lava in the crater during repose and an empty crater during repose, respectively. (c) RMS of the HHE, HHN and HHZ components filtered 0.5 to 4 Hz. Data gaps at LHR are marked (orange lines) and filled by seismic data from NUPH and HOPS, where the amplitude was amplified by a factor derived from a time period where LHR recorded. (d) Ground velocity in m/s corrected for noise. (e) Cycle duration, (f) episode duration and (g) repose time. The times of the inner crater collapse on 10 June (magenta star), the plume event on 2 July (red star), the partial crater collapse on 11 July (dark red star) and the detached moving crater rim (orange line) are marked. (h) Cumulative time of tremor (black) and repose (grey) from 2 May 2021.

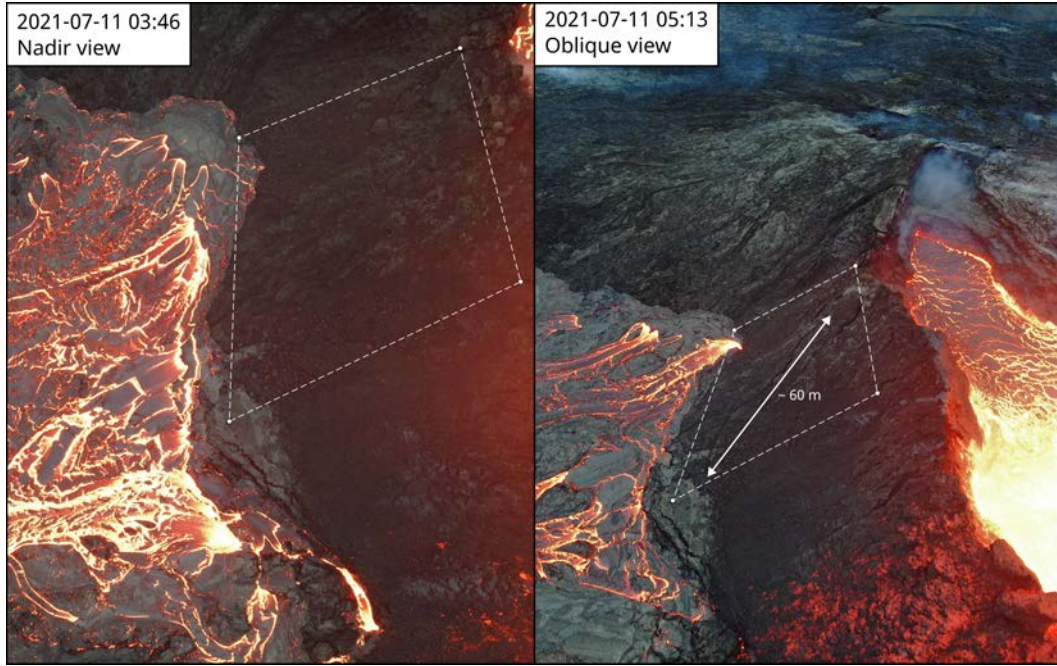


**Figure 3.** Evolution of cracks in the NE side of the crater on 11 July shortly before the collapse. Drone view of the NE side of the crater seen from the north. Cracks in the edifice are visible at 5:13 in the outlined area. The area enclosed by the dashed lines is approximately  $3500\text{ m}^2$ .

**Table 1.** Overview of terms used in manuscript and their definition.

Term	Definition
Tremor pulse	Tremor does not stop completely during the lull between subsequent tremor peaks
Tremor episode	Tremor stops completely during the lull between subsequent tremor peaks
Episode duration	Time between start and end of an episode
Repose time	Time between end of an episode to start of next one
Episode cycle duration	Time between start of an episode to start of next one
Sequence duration	Time between start of an hours-long ramp-shaped episode immediately followed by a series of minute-long episodes to the end of the last minute-long episode
Vent	Conduit feeding magma to the surface
Crater	Edifice above the pre-eruptive surface built by the lava effusion from a vent

**Phase III** lasts from 10:00 on 13 June 2021 to 23:00 on 5 July 2021. The cycle duration is quite heterogeneous. It begins on 13 June with  $3.5 \pm 0.5$  min long cycles that transition into continuous tremor at 15:56. The continuous tremor lasts until 0:57 on 2 July, when it abruptly stops. However, it is interrupted from time to time by 5 to 7 min long cycles e.g. between 12:22 and 18:57 on 25 June, 22:56 on 25 June and 8:13 on 26 June, 15:11 and 16:10 on 26 June, 6:52 and 7:50 on 27 June, 13:36 and 15:29 on 28 June, and 20:00 on 29 June and 4:48 on 30 June (Fig. 2e). Between 25 and 30 June episodes were on average 3 min long with on average 2 to 4 min long repose times. On 2 and 4 July two 38 and 30 h long episodes of larger seismic amplitude (Fig. 2f) are followed by 13 and 30 h long repose times, respectively (Fig. 2g). The seismic amplitude shows a bimodal distribution, reflecting the small amplitudes on 13 June and the 3 to 4 times larger amplitudes at the end of June (Suppl. Fig. 7).

### 4.3 Transition to Longer Episodes

**Phase IV** lasts from 23:00 on 5 July to 17:37 on 19 July and contains five 17 to 158 h long sequences (Fig. 2f). Each sequence begins with a 10 to 125 h long episode (Suppl. Fig. 6) followed by a 7 to 114 h long period with several minute-long episodes. The minute-long episodes are on average 3.5 to 8.5 min long. In the first sequence they decrease from 55 min to 6 min and then remain stable at 6 min. In the second sequence the episode duration increases from 3 to 8 min. After the collapse of the crater wall on 11 July (Fig. 3), the episode duration decreases to 3 min and then increases again to 7 min. In the third and fifth sequences, the episodes shorten from 14 to 3 min. The repose time between the end of one sequence and the beginning of the next is 6 to 30 h (Fig. 2g). Within the first sequence the repose time is about 9 min. Within the second sequence it increases from 0.7 to 14 min. After the collapse on 11 July (Fig. 3) the repose time decreased from 19 to 12 min. Within the third and fifth sequences, repose times are around 5 and 2 min. The first sequence on 7 and 8 July is interesting because its amplitude is about 10 times smaller than the amplitudes in the following episodes, but it lasts 5 to 12 times as long as the other 4 following sequences. Glow from the crater is visible on 7 and 8 July. The most dominant feature in Phase IV is a correlation between the episode duration and cycle duration (Suppl. Fig. 8).

**Phase V** begins at 17:37 on 19 July and contains 30 tremor cycles ranging from 17 to 65 h in duration. They are composed of 10 to 56 h long episodes that gradually increase in duration with time except for one episode from 5 August that is exceptionally long (Fig. 2f and Suppl. Fig. 6). The repose times are 7 to 38 h long (Fig. 2g). In terms of amplitude, the tremor episode on 3 August stands out, since it reached only a maximum amplitude that is 4 times smaller than all other episodes in that month.

The final **Phase VI** lasts from 14:24 on 2 September to 17:40 on 18 September and contains a 234.8 h long sequence of a 52.5 h long episode followed by a 121.8 h long period of several minute-long episodes. The minute-long episodes initially last 21 min and decrease exponentially to about 5 min within a few hours (Fig. 4c). Their duration remains around 5 min until the eruption ends. The sequence is preceded by a 212.3 h long repose time followed by 3 min long repose times on 14 September, which increase linearly to 11 min on 18 September. Similarly, the tremor amplitude increased linearly from 14 to 18 September. For the first 10 episodes, episode duration and cycle duration correlate. For the rest of the phase, only the repose time and the cycle duration correlate (Suppl. Fig. 10). The last hours of the effusive activity on 18 September from 9:30 to 18:00 (Fig. 4) broke the trend and the repose time dropped to less than 4 min (Fig. 4d), the seismic amplitude decreased (Fig. 4b) while three small sequences occurred. Each sequence started with 20 to 90 min long continuous tremor. The following minute-long episodes had a stable duration of 4 min each, followed by a 2 to 6 min long repose time.

Assessing the cumulative time of lava extrusion and repose between 2 May and 13 June, the system spent 12.2 more days in repose than in lava extrusion (Fig. 2h). The following 12 days continuous effusion is maintained until the cumulative time spent on

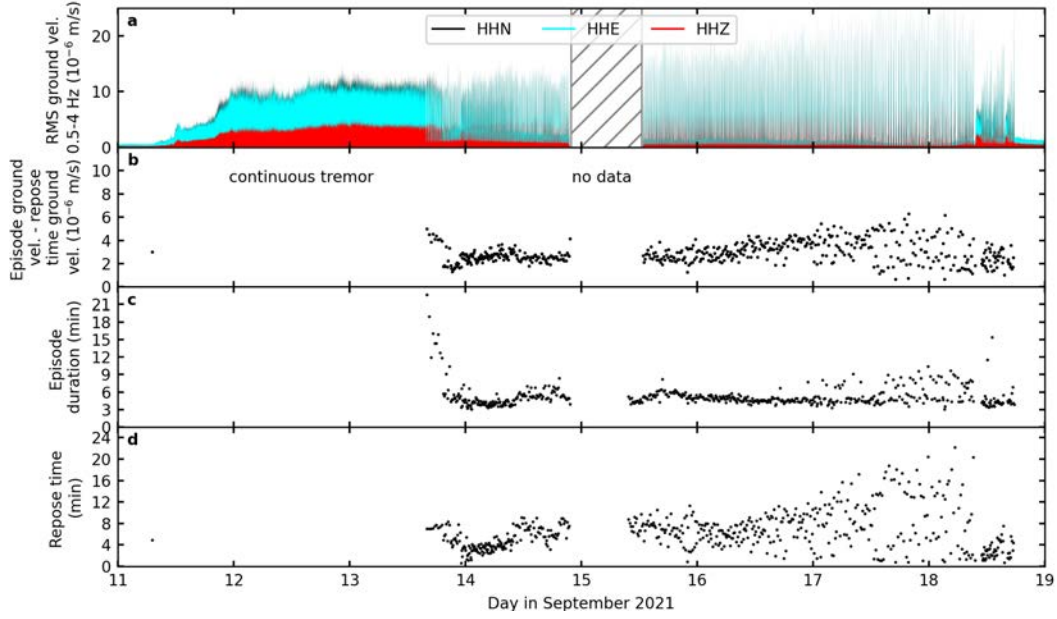


**Figure 4.** Episodic tremor pattern of the final sequence in September 2021. Same subfigures as in Fig. 2c-d, f-g. Hatched area indicates a data gap.

both is approximately equal. From 26 June the system spent more time in lava extrusion than in repose. On 2 September this reached 13.5 days more lava extrusion than repose, followed by 9 days of repose. The rate of tremor per month is stable in the first half of May and throughout July and August. In contrast, the system featured more repose time per month in May and less in July and August.

#### 4.4 Tremor Amplitude Increases at Slower Rates

Here, we assess the tremor increase rates of the ramp-shaped, hour-long episodes (Fig. 5). The tremor amplitude increases slowly over several hours and ends rapidly with a large variation in duration up to this point. Within the first hour after this rapid cessation of tremor, these hour-long episodes are often followed by one or more weak tremor bursts lasting a few minutes (Fig. 2f and Suppl. Fig. 11).

Of the five sequences in Phase IV, the first three increase rates are small, while the last two increase rates are about 2.5 times faster (Fig. 5c). The same increase rates are maintained for the first 5 episodes in Phase V (Fig. 5d). The next 6 episodes have 3 times slower increase rates (Fig. 5e), followed by two episodes with another 3 times slower increase rates (Fig. 5f).

The remaining 17 episodes (Fig. 5g-i) show a slow increase to  $3 \cdot 10^{-6}$  m/s and a gradual but faster increase to  $8.5 \cdot 10^{-6}$  m/s. The only exception is the last episode before the week-long repose interval. This episode begins on 1 September, rises to the first tremor amplitude level of  $3 \cdot 10^{-6}$  m/s, then rises exponentially to  $5 \cdot 10^{-6}$  m/s and then jumps to  $8.5 \cdot 10^{-6}$  m/s. This sudden amplitude increase is remarkable and unique.

The increase rate of the final episode on 11 September (Fig. 5j) is similar to the last ones in August, except for an increased tremor amplitude within the first hour and a longer duration of 2 days.

The maximum tremor amplitude in these hour-long sequences and episodes is reached at different points in time. While for the first 13 episodes in Phase IV the maximum tremor is reached towards the end of the episode, the last 17 episodes reach the maximum tremor about 6 to 8 h before the tremor stops.



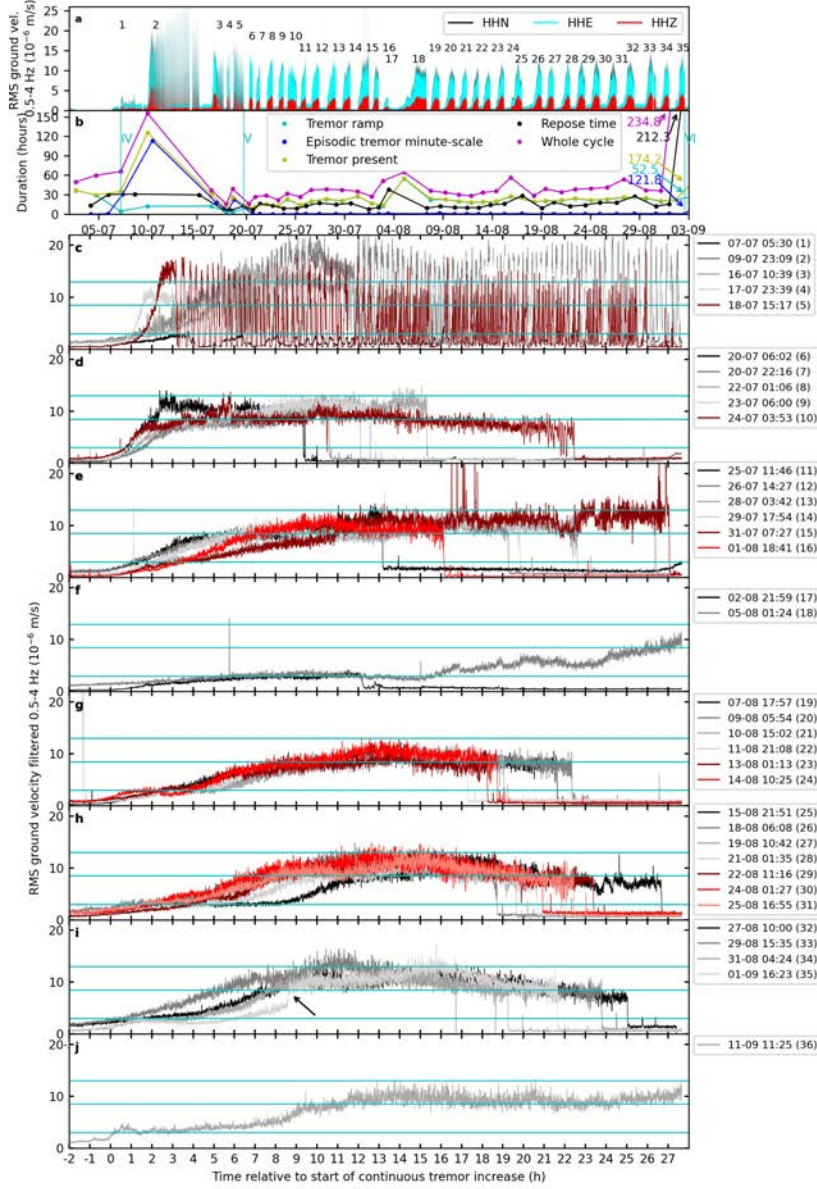


**Figure 5.** Changes in increase rates of the tremor amplitude during hour-long episodes. (a) RMS seismic ground velocities of the east (cyan), north (black) and vertical (red) components. (b) Duration of hour-long episodes, repose and cycle. Duration of periods with consecutive minute-long episodes. (c-j) Stacked RMS of the several hour-long tremor episodes from 6 July to 12 September 2021. We align the tremor at the beginning. Episodes from (c) 7 July to 19 July, (d) 20 to 24 July, (e) 25 July to 1 August, (f) 2 to 6 of August, (g) 7 to 14 August, (h) 15 to 26 August, (i) 27 August to 1 September and (j) 11 September. Horizontal cyan lines mark tremor amplitudes of 3, 8.5 and  $13 \cdot 10^{-6}$  m/s. The black arrow points to the sudden increase in tremor amplitude during the last episode before the one week-long repose time.

## 5 Discussion

### 5.1 Trends in Minute-long Episodes in the Context of the Crater, Vent and Magma Compartment

In the following discussion we assume a constant magma inflow rate, since the observed changes in magma discharge from May are within the range of the uncertainty (Pedersen et al., 2022; Thordarson et al., 2023).

McNutt and Nishimura (2008) reported a correlation between the cross-sectional area of the vent (conduit) and the tremor amplitude measured in reduced displacement. Along these lines, E. P. S. Eibl et al. (2023) suggested that the seismic amplitude during the Geldingadalir eruption reflects the width of the crack during effusion. It was likely thermally eroded and widened during May and in early June (E. P. S. Eibl et al., 2023; Lamb et al., 2022). We observe maximum seismic amplitudes in early June, between 7 and 19 July and from 13 to 18 September (Fig. 2d). In all these periods the minute-long episodes dominate. During the hour-long episodes, the seismic amplitude is smaller, possibly indicating that the crack is not opening as wide as during the minute-long episodes. This could be due to an increasing volume of material accumulating in the crater above the crack between 18 July and 3 September, or to more pressure associated with the minute-long episodes. In this context, the small tremor amplitude on 7 and 8 July could reflect a narrow crack, possibly blocked by collapsed material. However, we found no evidence of a collapse on 6 or 7 July.

Based on the episode durations from 2 May to 13 June, E. P. S. Eibl et al. (2023) suggested that a shallow magma compartment developed between 2 and 11 May with episodes up to 20 min long, and that its volume was stable from 11 May to 13 June with mostly 2.5 min long episodes. The minute-long episodes increased again to around 20 min and fluctuated rapidly from 7 to 19 July (Fig. 2e). In addition, the episode duration again correlated with the cycle duration (Suppl. Fig. 8a), which is similar to the trends observed by E. P. S. Eibl et al. (2023) from 2 to 11 May. We suggest that these patterns indicate a further modification and expansion of the shallow magma compartment. This could be triggered and modulated by the plume event on 2 July or the partial crater collapse on 11 July. During the first 10 episodes on 13 September, the episode duration decreased from 22 min to 6 min, similar to the trends on 2, 5 and 8 May (E. P. S. Eibl et al., 2023). This may indicate changes in a possible new shallow compartment due to the new magma path leading to the surface.

The repose time in May and June was interpreted in the context of the accumulation of outgassed material in the growing crater (E. P. S. Eibl et al., 2023). As the crater volume increased during July, we would expect to see a slight increase in the minute-long repose time. Indeed, we observe an increase to 20 min. However, we might expect an increase in repose time when the crater closed on all sides in early June, which is not visible. We might also expect a decrease when the crater wall partially collapsed on 11 July, and indeed the repose time decreased to about 1 min after the collapse, while within 1 day it increased back to 20 min, although the detached block continued to move for several days.

### 5.2 Order of Magnitude Changes in Episode Duration Reflect Open and Semi-closed Vent System

The episode duration increased by two orders of magnitude from the minute to the hour scale on 25 June. For the following discussion we consider that the minute-long episodes reappear in early July at Vent-5 and in September at the new opening, and that the shape of the hour-long tremors on 2 and 4 July is more similar to the continuous tremor in June than to the hour-long episodic patterns in July and August.

If we interpret the episode duration in terms of the size of the magma compartment, it must have increased significantly between 25 June and 20 July, when the hour-long tremor episodes occur and the minute-long episodes at Vent-5 occur for the last time.



The plume event on 2 July and the partial collapse of the crater on 11 July (Fig. 3) may have started to expand or merge with a larger reservoir between 2 and 20 July. There is no evidence for extension in the deformation data (Geirsson et al., 2022). Greenfield et al. (2022) reported a deep long period (DLP) event swarm in late June and in July 2021 that is aligned with the transition to hour-long episodes. These DLP events could indicate changes in CO<sub>2</sub>-rich fluids or the movement of magma about 5 km above the Moho in the same time window. From 20 July, the hour-long tremor episodes dominate, possibly reflecting a larger reservoir. During the week-long repose time in early September, the old pathway closed and a new one formed, that is possibly linked to a new small magma compartment. This small compartment could be reflected in the reappearing minute-long episodes. At Etna, Viccaro et al. (2014) suggested that short strombolian phases before paroxysms were associated with gas injections into the residing system and longer strombolian phases before paroxysms were associated with gas-rich magma recharge. During the Geldingadalir eruption, the magma composition had shifted to the enriched olivine tholeiite by 2 May and from then on the composition of the erupted magma remained unchanged until the end of the eruption (Bindeman et al., 2022).

We think that it is more likely that a reservoir of constant size was maintained from 11 May until September 2021. In this scenario, the hour-long tremor episodes could reflect its size, while the hour-long repose time represents a period with a semi-closed vent and lava completely drained from the crater edifice. During the minutes-long tremor episodes, a lava pond remains in the crater during repose in May, and we propose that this may have been the case from 7 to 19 July and from 13 to 18 September. In such a system, where a lava pond is connected to the shallow reservoir and cyclic degassing (E. P. S. Eibl et al., 2023; Scott & Al., 2023) drives lava fountaining episodes, lava might drain from the pond into the lava flow field during the minute-long repose time. The episode duration might hence be shorter in May as some of the volume drains seismically silent and less material can accumulate. A modification of the shallow conduit system may have disrupted the connection between the shallow magma compartment and the lava pond in the crater, changing the drainage pattern. This could have been caused by the plume event on 2 July and the partial collapse of the crater on 11 July (Fig. 3), and further evidence for the modification is also provided by the increased episode duration. The increased episode duration in early May was interpreted by E. P. S. Eibl et al. (2023) as a modification in a shallow magma compartment.

Interestingly, we also find a two order of magnitude increase in repose time from 2 July. Dominguez et al. (2016) found a correlation between repose time and magma viscosity. In the context of a two order of magnitude increase in repose time, it seems unlikely that this is driven by an order magnitude increase in viscosity especially since the shorter repose times reappear.

We suggest that these two orders of magnitude difference in repose time reflect two different states of the system. Minutes-long repose times reflect an open vent system where lava residing in a lava pond in the crater is linked to the shallow magma compartment. Repose times are shorter as lava extrusion and effusion can start more easily when degassing of magma starts. Hour-long repose times reflect a semi-closed vent system with no lava residing in the crater during the repose time. For lava extrusion and effusion, the vent must be reopened, and the vent closure may push some remaining magma out of the way, causing the tremor bursts within the first hour after the rapid tremor end (Suppl. Fig. 11). Smaller increases in minute-long repose times e.g. from 3 to 11 min from 14 to 18 September or throughout May, are more likely to reflect the amount of accumulated outgassed material remaining in the crater, as suggested by E. P. S. Eibl et al. (2023).

Increases in duration of an order of magnitude or more are uncommon, short-lived and rarely interpreted in the literature. On Etna, Andronico et al. (2021) published a complete list of lava fountain successions from 1986 to 2021. The repose times from one fountain succession to the next fountain succession are an order of magnitude greater than the repose time within a succession. Within a succession, only one succession from

2011 to 2012 showed a short-lived increase of one order of magnitude. Alparone et al. (2003) studied a succession on Etna in 2000 in more detail and reported a sustained increase in repose time from  $10^3$  to  $10^4$ , maintained for four consecutive fountaining episodes in late February. From 23 February they reported a small fissure opening at the base of the cone, until late April when it closed. This time period featured slightly longer episode duration and an order of magnitude longer repose time. The fissure may have reduced the amount of outgassed material accumulated in the cone, in contrast to our interpretation. Privitera et al. (2003) reported an order of magnitude increase in cycle duration for only 1 out of 16 episodes on Etna in 1989. From 1983 to 1986 Heliker and Mattox (2003) reported an overall decrease in episode duration from 12 days to 0.5 days during the Pu‘u ‘Ō‘ō-Kūpaianaha eruption, except for the first episode and small fluctuations around the trend. A sudden order of magnitude increase in episode duration from 0.4 to 16 d and in repose time from 8 to 120 d was short-lived and maintained for only one episode (episode 35a and 7, respectively). The increase in duration was associated with a fissure opening on the uprift side of the Pu‘u ‘Ō‘ō. Spampinato et al. (2015) observed on Mt. Etna in 2013 that the repose times increased from 1 d to 18 d and then decreased to 2 d again. Calvari et al. (2011) reported that the number of explosions in a 15 min long time window increased from 1 to 80 in January 2011, and that consequently the cycle duration gradually decreased by almost two orders of magnitude. Patrick et al. (2011) reported two sudden decreases from 25 to 2 spattering events per day in a perched lava channel at Kilauea. None of these examples reported sustained increases of more than an order of magnitude, such as we observed during the Geldingadalir eruption from July 2021.

During the Geldingadalir eruption, the episode duration is in May to June two orders of magnitude smaller than at Etna ( $10^1$  compared to  $10^3$ ) and, when the longer episodes start in late June (range of  $10^3$ ), comparable to Etna. The magma compartment driving the effusion could therefore be similar in size to Etna, if our hypothesis that the tremor duration is related to the magma compartment size is correct. The repose times at Geldingadalir range from  $10^1$  to  $10^3$ , while those on Etna range from  $10^3$  to  $10^5$ . This could reflect different inflow rates, conduit or crater dimensions.

### 5.3 Transitions between periods of continuous effusion, minute-long episodes and hour-long episodes

We define 6 phases during this eruption. From each phase to the next, we observe transitions from (i) continuous tremor to (ii) minute-long episodic tremor to (iii) continuous tremor and minute- and hour-long episodic tremor to (iv) one hour-long episode followed by several minute-long tremor episodes to (v) hour-long episodic tremor to (vi) one hour-long episode followed by several minute-long tremor episodes (Fig. 2c). To our knowledge there is no other eruption with similarly strong changes in eruption style.

However, when looking at the trend created by the number of events per time unit (Fig. 2b), we find a similarity to Etna volcano. At Geldingadalir the events are closely, moderately, widely and closely spaced in Phase II (May to June), Phase III and IV (early to mid-July), Phase V (mid-July to early September) and Phase VI (after 12 September), respectively. Similar trends in the temporal spacing of events are visible on Etna from September 1998 to February 1999, from January 2011 to April 2012 and from February to April 2013 (Andronico et al., 2021). The most similar succession is the lava fountain succession from January to July 2000 on Etna. Alparone et al. (2003) divided 64 lava fountains into a first stage featuring up to 3 events/ day and a second stage with temporarily more distant spaced events. They show similar sudden kinks in the event number with time curve (their figure 6) and maintain the new event number per day for several episodes. Both successions last 6 months, but the event number is significantly higher at Geldingadalir.

Andronico and Corsaro (2011) analysed chemical data from the Etna fountain succession in 2000 and argued that in the first stage a more primitive, volatile-rich magma

reached the residing magma in the reservoir beneath the SE crater. The magmas mixed and exsolved gases from the new magma batch accumulated, triggering the lava fountains in quick succession. In stage 2 on Etna the mixing continued and eventually the contribution of new magma ceased, and the reservoir composition returned to the evolved composition it had before the onset of the lava fountaining. Since the most mafic magma erupted between 15 and 17 May 2000, mixing was well advanced at that time. Subsequently, the supply of new magma from depth ceased, coinciding with a time period of a chaotic succession of tower, bell and ramp-shaped tremor on Etna. Following their argument for the Geldingadalir eruption, we might suggest that after 11 September the supply of magma from depth decreased slightly, leading to the mixed succession. Since there is a remarkable uniformity in the bulk geochemistry of the products from mid-May onwards (Bindeman et al., 2022), we currently find no evidence for a mixing of a residing magma with an ascending, deeper magma to explain the changes in repose time and episode duration. Evidence for rapid magma mixing has only been found in April 2021 of the Geldingadalir eruption (Halldórsson et al., 2022; Bindeman et al., 2022). Unfortunately, the evolution of the event number over time on Etna shows two other kinks that are not discussed further in the context of the magma hypothesis proposed by Andronico and Corsaro (2011).

During the 2021 La Palma eruption Romero et al. (2022) studied the formation and collapse of a cone. This changed the vent geometry and was followed by a pause in the eruption possibly due to rapid emptying of the shallow reservoir or blocking of the vent. The lava fountain height was not affected, and on a longer time scale the collapse did not influence the effusion pattern. During the Geldingadalir eruption, the circular collapse inside the crater on 10 June at 4:10:18 shortened the repose time and reduced the seismic amplitude (E. P. S. Eibl et al., 2023). Subsequently, the episodic pattern was less pronounced, and part of the vent may have become blocked, allowing a transition back to continuous effusion. If this reduces the outflow rate, degassing may keep up with the effusion and allow a continuous outflow.

Between 25 and 30 June, the continuous effusion may have thermally eroded the vent enough (indicated by an increasing seismic tremor amplitude) to leave the system in a delicate balance between continuous and episodic effusion. Further erosion could increase effusion rates and restart the episodic pattern, driven by an effusion rate that is faster than the rising rate of the deep magma.

Continuous tremor resumed when the cumulative sum of tremor time lagged 12.2 days behind the cumulative sum of the repose times. Strikingly, this continuous effusion continued until the cumulative tremor time had caught up with the cumulative repose time. At this point in late June, it transitioned back to episodic, featuring the same cumulative tremor time per month as in May. This suggests that the process/ nozzle controlling the time spent on effusion did not change. The repose time per month is greater in May than in July and August. Given that the inflow rate was unchanged, we propose that this reflects the open vent system and silent flow of lava from the lava pond during repose in May to mid-June, while a semi-closed vent system in July and August could build up sufficient pressure faster, resulting in a shorter repose period. This is consistent with the observation that in June and until 20 July magma remained in the crater during the repose period and from 26 July the crater emptied completely during the repose period. It is noteworthy that the 1-week long repose period occurred when the cumulative tremor time was more than 2 weeks ahead of the cumulative repose time. For a stable effusion pattern, it hence seems important to keep a balance between effusion and repose time. During minute-long episodes, the tremor duration influenced the following repose time. For example, the longer the tremor lasted, the longer it took for the system to recharge afterwards. As the magma compartment was probably connected to the lava residing in the crater bowl, a cyclic degassing process drove the effusion pattern. In such a system, more gas might escape and maintain an effusion period for longer, triggering a longer repose. At Geldingadalir, however, the opposite was true during the hour-long episodes. The system featured a longer repose time before a longer tremor episode.

As the connection between the shallow magma compartment is closed and no lava remains in the crater bowl, the system may need to build up more pressure before it can resume effusion, leading to longer repose times before longer episodes. In this context, the last tremor episode before the week-long hiatus is interesting. It takes longer for the tremor to increase and finally jumps to a larger tremor amplitude (black arrow in Fig. 5i). This may reflect how difficult it was to reopen the crack. It managed to effuse for a few hours, but then had to rest longer before enough pressure and material had accumulated to start the final sequence in mid-September. Alparone et al. (2003) reported for Etna that the previous repose time correlated with the duration of the next episode. But in contrast to our study, Etna volcano spent more time per month in repose than effusion.

#### 5.4 Shape of the Tremor from Rectangle, to Bell to Ramp

Tremor can be episodic (E. P. Eibl, Bean, Vogfjörð, et al., 2017; E. P. S. Eibl et al., 2023; Patrick et al., 2011; Alparone et al., 2003; Heliker & Mattox, 2003; Privitera et al., 2003; Thompson et al., 2002; Carbone et al., 2015; Moschella et al., 2018) and the shapes of successive tremor episodes are often similar. For example, the time period in February 2000 on Etna featured only bell-shaped tremor. In April and the first half of May 2000, only ramp-shaped tremors occurred during lava fountaining episodes (Alparone et al., 2003). A succession of only ramp-shaped tremor was also documented during the caldera collapse at Piton de la Fournaise in 2007 (Staudacher et al., 2009).

However, the lava fountain succession in 2000 on Etna produced a tremor pattern in March consisting of one ramp- and several bell-shaped tremors. From 17 May, the succession contained even more chaotic tremor shapes (tower, ramp, bell and unclassifiable shapes) in random order (Alparone et al., 2003). Similarly, Viccaro et al. (2014) reported the tremor amplitude shape of 25 fountaining events in 2011 and 2012 on Mt. Etna, without showing a clear succession in terms of the shape of the tremor amplitude or association with episode duration or repose times. The other mentioned studies did not describe the tremor shape in sufficient detail to assess the similarity of the episodes.

Throughout the Geldingadalir eruption, we observe transitions from rectangle- to bell-shaped tremor during minute-scale tremor. On 30 June, we observe the first few minute-long ramp-shaped tremor. From 7 July onwards, the duration of the ramp-shaped tremors increase to hour-scale. The last three ramp-shaped tremors on 18 September are again of minute duration, which could be associated with less magma coming up from depth. We did not notice any specific event around the occurrence of the first ramp-shaped tremor. This is in contrast to Alparone et al. (2003), who observed a first ramp-shaped tremor just before the opening of a fissure at the base of the cone, which changed the eruptive dynamics. However, although we did not observe a fissure opening, we did observe the plume event 2 days later, which possibly modified the shallow conduit.

According to Alparone et al. (2003), a ramp-shaped tremor reflects initial Strombolian activity during increase, a fountaining phase during maximum tremor amplitude, and a sudden decrease in tremor amplitude associated with Strombolian activity following the fountaining. Here we observe no Strombolian activity and an increase in bubble size and in the abundance of bubbles bursting in the lava pond. The tremor decrease happens within a few minutes and coincides in time with a sudden decrease in pond height and the eruption end (e.g. no more visible gas plume).

During bell-shaped episodes, tremor increased over several minutes during the Geldingadalir eruption, and during ramp-shaped tremor it increased over several hours. McNutt and Nishimura (2008) reported exponential increases in tremor from 5 min to 1 d and exponential decreases at the end of eruptions lasting from 8 min to 14 d. Our decreases during bell-shaped tremor are a few minutes long and hence shorter. Viccaro et al. (2014) interpreted the ramp-shaped tremor as gas-rich magma recharge and long effusion, and the bell-shaped tremor as gas injections into the residing system and short effusion. During these episodes, the mean effusion rates ranged from 64 to 980  $m^3/s$  (Behncke et al., 2014). This could be true for systems that feature one shape and then transition to the

other shape, or a spread in effusion rates. However, during the Geldingadalir eruption such an explanation seems unlikely given the many transitions in shape and the overall low and steady effusion rates. In contrast, during the episodic vent activity, magma effusion was high, at least at peak intensity and at times vigorous. The mechanism controlling this decoupling between the more immediate and vigorous vent behavior (i.e., the episodes) and the more prolonged and steady lava effusion is the key to understanding the episodicity of the 2021 Geldingadalir eruption. It is likely that the ramp-shaped tremor reflects the closed vent between the crater and the shallow magma compartment, which is more difficult to reopen for effusion, while the rectangle- and bell-shaped tremor occur in an open system with lava in the crater bowl, which can more easily restart the effusion.

In Phase IV, a ramp-shaped tremor is followed by several bell-shaped tremors. The tremor amplitude of the first three ramps increases more slowly than that of the last two ramps. This coincides with the movement of the detached part of the crater rim. Once the part stops moving, the tremor amplitude increases faster. This suggests that during the first three sequences the energy of the degassing magma was partly used to move the block and partly to open the crack. When the crater rim solidified again, the crack could be reopened faster.

In Phase V, the tremor amplitude increases at a similar rate for 5 to 6 episodes and then the rate suddenly decreases for the next 5 to 6 episodes. Only from 7 August is there a similar rate of increase in tremor amplitude from one episode to the next. The decrease of the increase rates of the tremor amplitude might be related to the accumulation of more outgassed material in the crater, leading to a slower opening of the closed vent. While Alparone et al. (2003) could relate the rise time from start to maximum tremor amplitude to the total duration of the tremor episode, our rise times cannot be used to infer the duration (e.g. Fig. 5c). Further classifying the tremor increase rates during 25 paroxysms in 2011/12, Viccaro et al. (2014) observed two different tremor shapes, where slow tremor increase rates defined a ramp-shaped tremor and fast increase rates a bell-shaped tremor. However, Viccaro et al. (2014) did not observe any systematic change in the tremor increase rates from one episode to the next one. Here, both the ramp- and bell-shaped tremor featured variable increase rates, but the same decrease rates at the end of a tremor episode. It remains a puzzle of why there is no gradual but step-like decrease in the tremor increase rates.

## 6 Implications and Outlook

The 2021 Geldingadalir eruption in the Fagradalsfjall Fires featured a unique and unprecedented succession of episodic tremor. After about 6 weeks of continuous lava effusion, 8696 tremor episodes occurred between 2 May and 18 September 2021. The most striking feature is a two order of magnitude increase in effusion duration and repose time from July despite a constant lava effusion rate. We interpret the several-minute long tremor episodes in the context of an open vent system where a lava pond remains in the crater during the repose time. This lava pond is always linked to a shallow magma compartment that drives an episodic degassing process and lava fountaining in the vent. The several-hour long tremor episodes are interpreted in the context of a semi-closed vent system, where no lava remains in the crater during repose time.

The system likely transitions from one state to the other as a result of major collapses or plume events, and further analysis may reveal their detailed effects on the system. These events may also have affected the amplitude increase rates of the ramp-shaped tremor, and hence the rate at which the lava extrusion intensifies.

Finally, if we look at the cumulative time spent by the system in a lava extrusion compared to the repose state, we see that they keep up with each other. After an episodic lava extrusion in May and early June, where the system spent more time in repose than in effusion, the system maintained continuous effusion to catch up in June. Conversely, the system spent more time in the lava extrusion state in July and then featured a 1-week repose time in September before the final eruptive sequence. This might have implications for monitoring events that feature such episodic patterns.

## Open Research Section

Seismic data from station NUPH are available via GEOFON (E. P. S. Eibl, Hersir, et al., 2022). The list of start and end times of tremor episodes until 13 June is available via GFZ Data Services (E. P. S. Eibl, Roskopf, et al., 2022). Further material will be made available during the review process.

## Acknowledgments

We thank Friðgeir Pétursson, Rögnvaldur Línal Magnússon, Thorbjörg Ágústsdóttir at ÍSOR and Daniel Vollmer at the University of Potsdam for technical support in the field. We thank Sebastian Heimann for programming support and Alea Joachim for creating and checking markers. We thank Sigurður Þór Helgason for collecting the drone data used in this study. We thank Brett Carr and Chris Hamilton for access to drone data for contextual purposes. Furthermore, we acknowledge Mila for providing electrical power for seismic station LHR on Langihryggur. The authors acknowledge that they received no funding in support for this research.

Author contribution:

Conceptualization: EPSE

Data collection: EPSE, EAG, GPH, TT, AH, WWM

Methodology: EPSE, WWM

Investigation: EPSE, TT, WWM

Visualization: EPSE, WWM, EAG

Writing—original draft: EPSE

Writing—review and editing: EPSE, TT, WWM, EAG, AH, GPH

## References

- Aki, K., & Koyanagi, R. (1981). Deep Volcanic Tremor and Magma Ascent Mechanism Under Kilauea, Hawaii. *J. Geophys. Res.*, *86*(B8), 7095–7109. doi: 10.1029/JB086iB08p07095



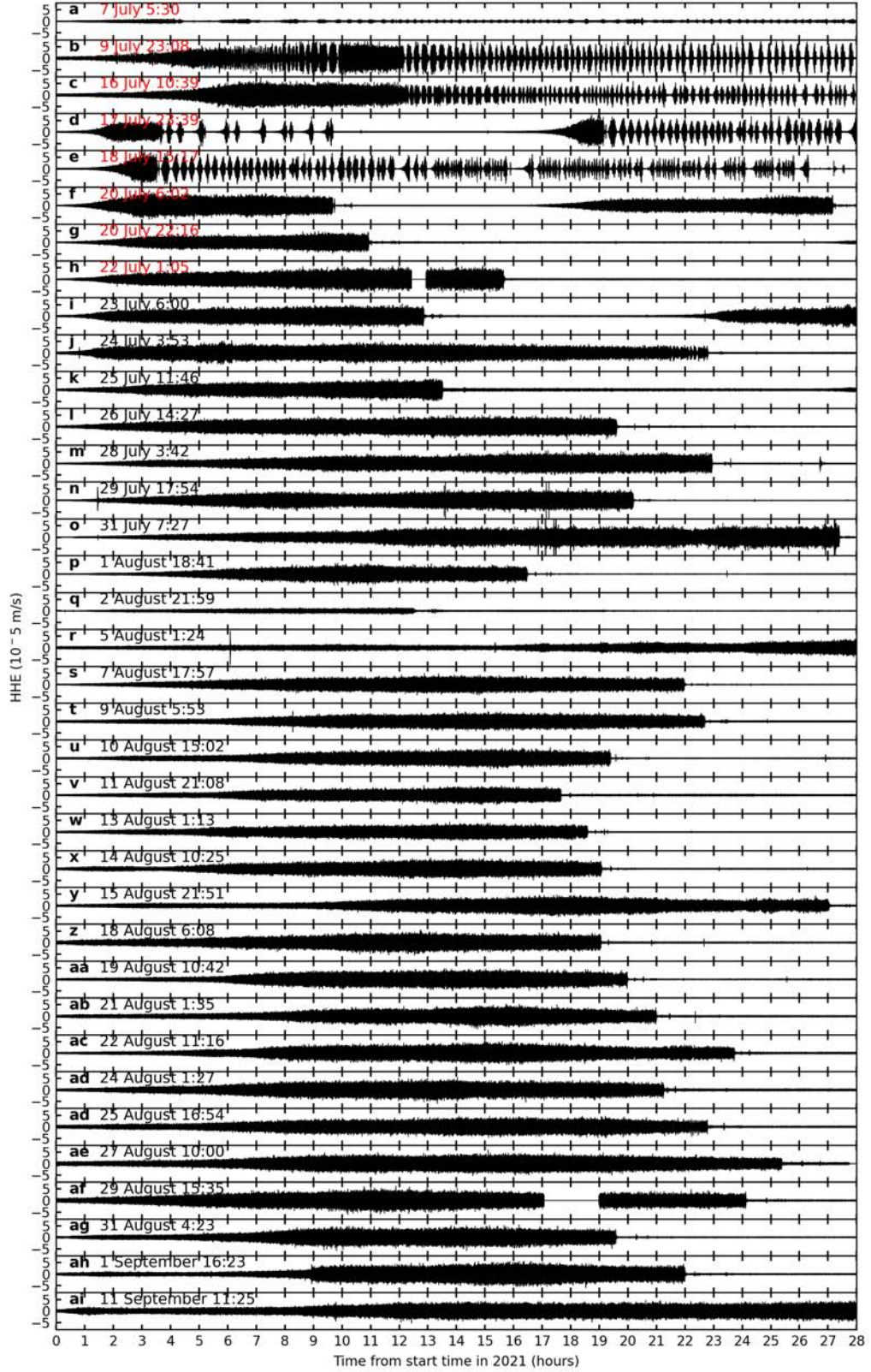


**Figure 6.** Seismograms of the ramp-shaped, hour-long tremor episodes. Data from 7 July to 29 August was filtered from 0.5 to 5 Hz in 30 hour long time windows. Start time of the time windows as indicated in the subfigure.

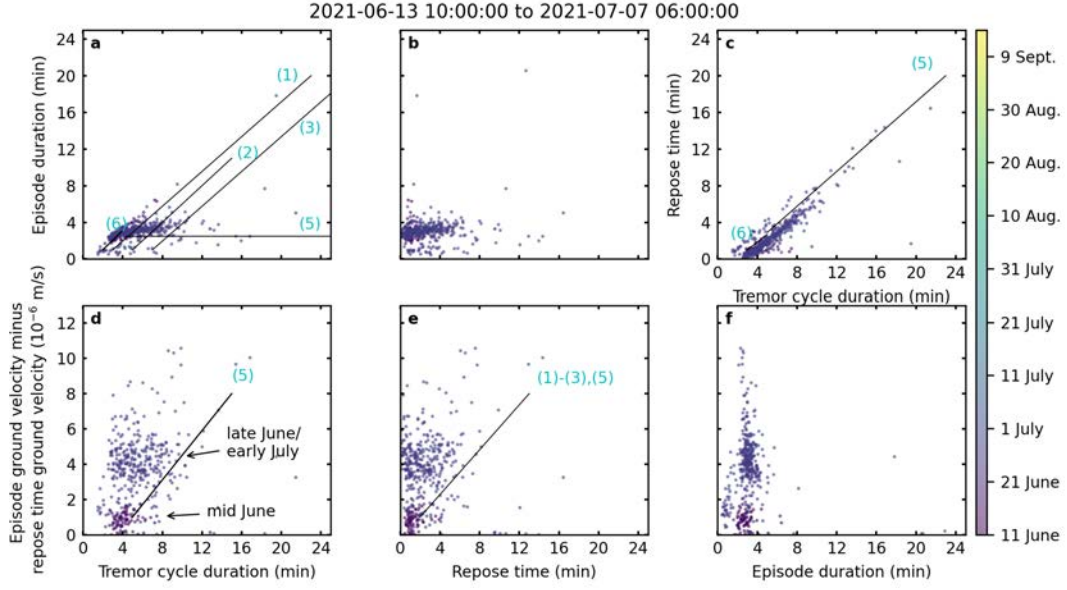


**Figure 7.** Correlation pattern of episode duration, repose time, cycle duration and tremor amplitude in Phase III similar to figure 5 in E. P. S. Eibl et al. (2023). (a-b) Correlation of episode duration with (a) cycle duration and (b) repose time. Colors indicate the time. The labelled black lines highlight the correlation trends in Periods 1 to 3, 5 and 6 in all subfigures as identified by E. P. S. Eibl et al. (2023). (c) Correlation of repose time and cycle duration. (d-f) Correlation of episode ground velocity corrected for wind noise and (d) cycle duration, (e) repose time and (f) episode duration.

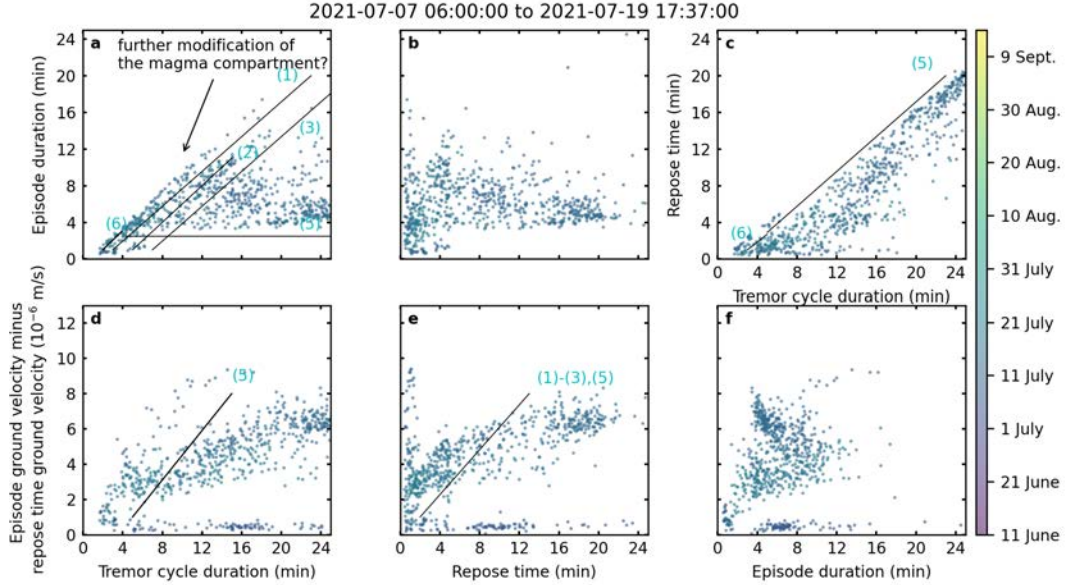


**Figure 8.** Same as Suppl. Fig. 7 for episodic behaviour in Phase IV.

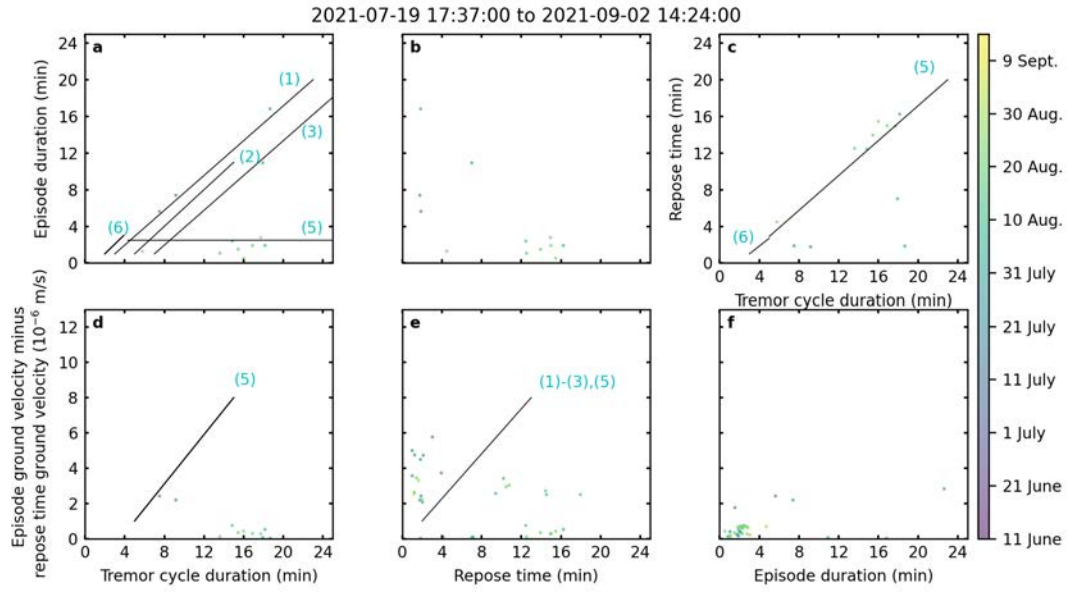


**Figure 9.** Same as Suppl. Fig. 7 for episodic behaviour in Phase V.

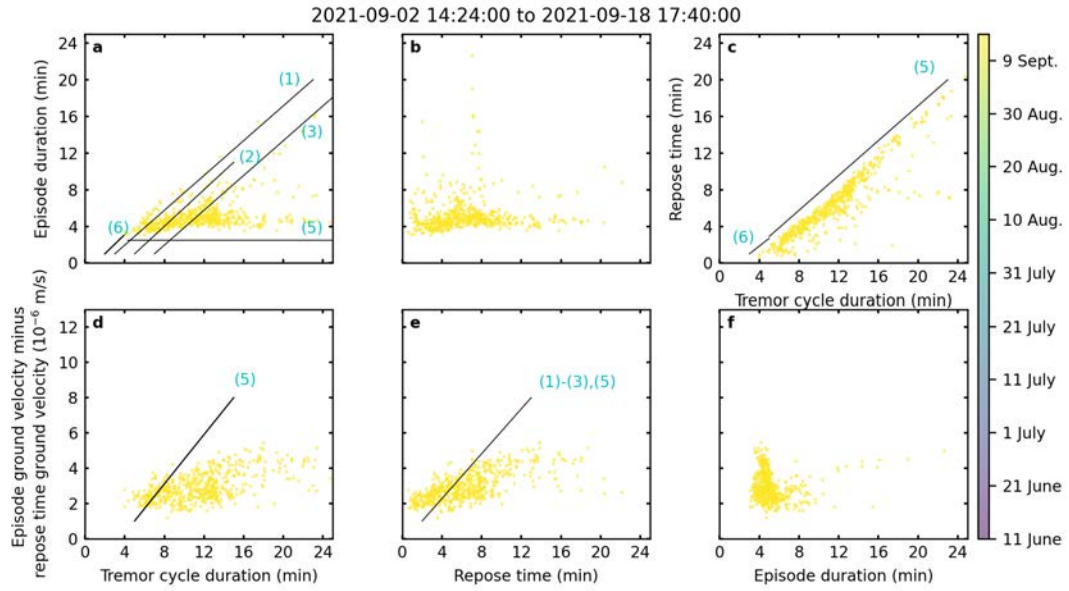


**Figure 10.** Same as Suppl. Fig. 7 for episodic behaviour in Phase VI.



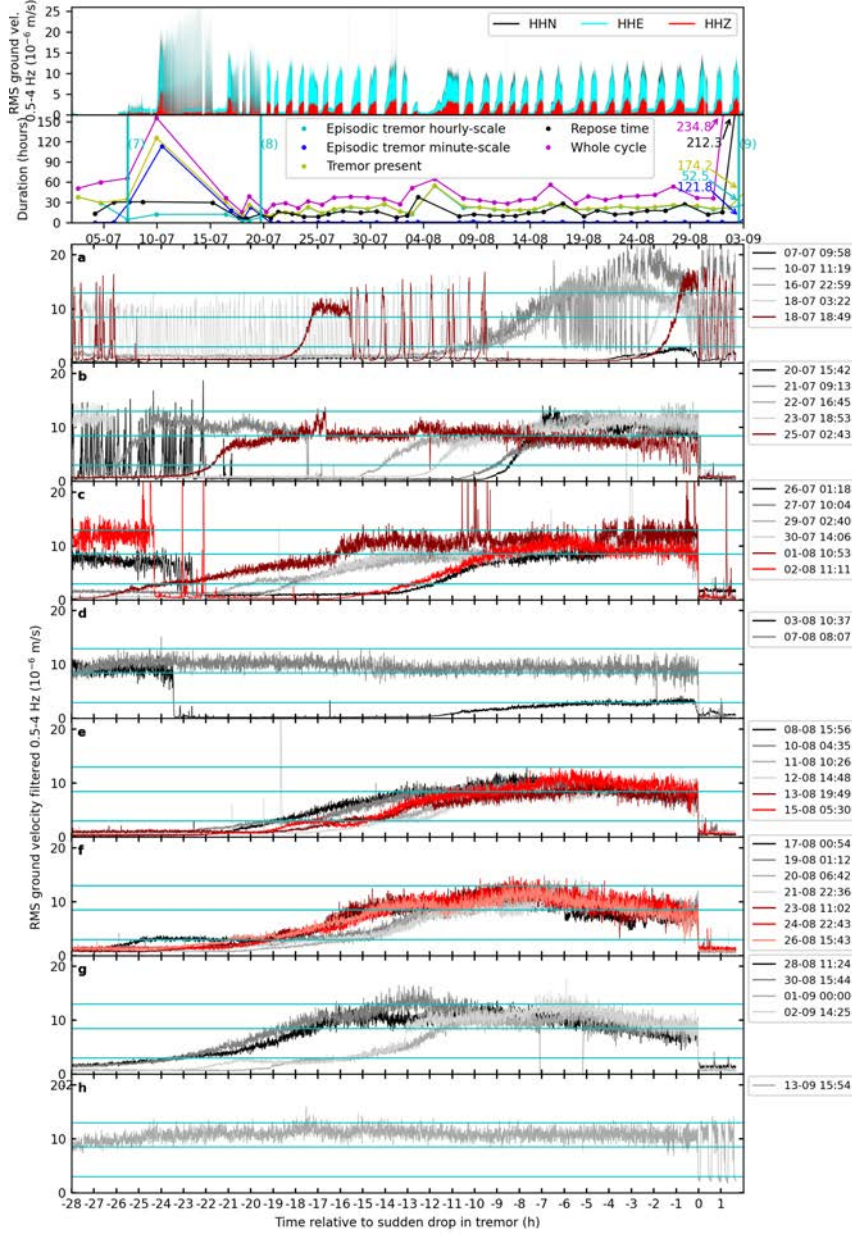


**Figure 11.** Hour-long, ramp-shaped tremor aligned at the rapid tremor end. Due to the short repose times between 7 July and 3 August some previous tremor episodes are also visible between hours -28 and -9 in contrast to Fig. 5. Note the weak tremor bursts in the first hour following the rapid tremor decrease.

- Allard, P., La Spina, A., Tamburello, G., Aiuppa, A., Coquet, A., Brenguier, F., ... Staudacher, T. (2011). First cross-correlated measurements of magma dynamics and degassing during a dyke eruption at Piton de la Fournaise hot spot volcano, Reunion Island. In *American geophysical union, fall meeting 2011*.
- Alparone, S., Andronico, D., Lodato, L., & Sgroi, T. (2003). Relationship between tremor and volcanic activity during the Southeast Crater eruption on Mount Etna in early 2000. *Journal of Geophysical Research: Solid Earth*, 108(B5), 1–13. Retrieved from <http://doi.wiley.com/10.1029/2002JB001866> doi: 10.1029/2002JB001866
- Andronico, D., Cannata, A., Di Grazia, G., & Ferrari, F. (2021). The 1986–2021 paroxysmal episodes at the summit craters of Mt. Etna: Insights into volcano dynamics and hazard. *Earth-Science Reviews*, 220, 103686. Retrieved from <https://www.sciencedirect.com/science/article/pii/S0012825221001872> doi: <https://doi.org/10.1016/j.earscirev.2021.103686>
- Andronico, D., & Corsaro, R. A. (2011). Lava fountains during the episodic eruption of South-East Crater (Mt. Etna), 2000: Insights into magma-gas dynamics within the shallow volcano plumbing system. *Bulletin of Volcanology*, 73(9), 1165–1178. doi: 10.1007/s00445-011-0467-y
- Battaglia, J., Aki, K., & Staudacher, T. (2005a). Location of tremor sources and estimation of lava output using tremor source amplitude on the Piton de la Fournaise volcano: 2. Estimation of lava output. *Journal of Volcanology and Geothermal Research*, 147(3-4), 291–308. doi: 10.1016/j.jvolgeores.2005.04.006
- Battaglia, J., Aki, K., & Staudacher, T. (2005b). Location of tremor sources and estimation of lava output using tremor source amplitude on the Piton de la Fournaise volcano: 2. Estimation of lava output. *Journal of Volcanology and Geothermal Research*, 147(3-4), 291–308. doi: 10.1016/j.jvolgeores.2005.04.006
- Behncke, B., Branca, S., Corsaro, R. A., De Beni, E., Miraglia, L., & Proietti, C. (2014). The 2011–2012 summit activity of Mount Etna: Birth, growth and products of the new SE crater. *Journal of Volcanology and Geothermal Research*, 270, 10–21. Retrieved from <http://dx.doi.org/10.1016/j.jvolgeores.2013.11.012> doi: 10.1016/j.jvolgeores.2013.11.012
- Beyreuther, M., Barsch, R., Krischer, L., Megies, T., Behr, Y., & Wassermann, J. (2010). ObsPy: A Python Toolbox for Seismology. *Seismological Research Letters*, 81(3), 530–533. Retrieved from <http://srl.geoscienceworld.org/cgi/doi/10.1785/gssrl.81.3.530> doi: 10.1785/gssrl.81.3.530
- Bindeman, I., Deegan, F., Troll, V., Thordarson, T., Höskuldsson, A., Moreland, W., ... Walter, T. (2022). Diverse mantle components with invariant oxygen isotopes in the 2021 Fagradalsfjall eruption, Iceland. *Nature Communications*.
- Calvari, S., Salerno, G. G., Spampinato, L., Gouhier, M., La Spina, A., Pecora, E., ... Boschi, E. (2011). An unloading foam model to constrain Etna’s 11–13 January 2011 lava fountaining episode. *Journal of Geophysical Research: Solid Earth*, 116(11). doi: 10.1029/2011JB008407
- Carbone, D., Zuccarello, L., Messina, A., Scollo, S., & Rymer, H. (2015, dec). Balancing bulk gas accumulation and gas output before and during lava fountaining episodes at Mt. Etna. *Scientific Reports*, 5. doi: 10.1038/srep18049
- Coppola, D., Piscopo, D., Staudacher, T., & Cigolini, C. (2009). Lava discharge rate and effusive pattern at Piton de la Fournaise from MODIS data. *Journal of Volcanology and Geothermal Research*, 184(1-2), 174–192. doi: 10.1016/j.jvolgeores.2008.11.031
- Çubuk-Sabuncu, Y., Jónsdóttir, K., Caudron, C., Lecocq, T., Parks, M. M., Geirsson, H., & Mordret, A. (2021). Temporal seismic velocity changes during the 2020 rapid inflation at Mt. Porbjörn-Svartsengi, Iceland, using seismic ambient noise. *Geophysical Research Letters*, 48(11), 1–10. doi:

- 10.1029/2020GL092265
- Dominguez, L., Pioli, L., Bonadonna, C., Connor, C. B., Andronico, D., Harris, A. J., & Ripepe, M. (2016, jun). Quantifying unsteadiness and dynamics of pulsatory volcanic activity. *Earth and Planetary Science Letters*, 444, 160–168. doi: 10.1016/j.epsl.2016.03.048
- Eaton, J. P., Richter, D. H., & Krivoy, H. L. (1987). Cycling of magma between the summit reservoir and Kilauea Iki lava lake during the 1959 eruption of Kilauea Volcano [abs.]. In R. W. Decker, W. T. Wright, & P. H. Stauffer (Eds.), *Abstract volume* (p. p. 60). U.S. Geol. Surv. Prof. Pap., 1350.
- Eibl, E. P., Bean, C. J., Jónsdóttir, I., Höskuldsson, A., Thordarson, T., Coppola, D., ... Walter, T. R. (2017). Multiple coincident eruptive seismic tremor sources during the 2014–2015 eruption at Holuhraun, Iceland. *Journal of Geophysical Research: Solid Earth*, 122(4), 2972–2987. doi: 10.1002/2016JB013892
- Eibl, E. P., Bean, C. J., Vogfjörð, K. S., Ying, Y., Lokmer, I., Möllhoff, M., ... Pálsson, F. (2017). Tremor-rich shallow dyke formation followed by silent magma flow at Bárðarbunga in Iceland. *Nature Geoscience*, 10(4), 299–304. doi: 10.1038/ngeo2906
- Eibl, E. P. S., Hersir, G. P., Gudnason, E. Á., & Péturson, F. (2022). 2-year seismological experiment near Fagradalsfjall, Reykjanes peninsula in 2021/22. *GFZ Data Services. Other/Seismic Network*. doi: 10.14470/4S7576570845
- Eibl, E. P. S., Roskopf, M., Sciotto, M., Currenti, G., Di Grazia, G., Jousset, P., ... Weber, M. (2022). Performance of a Rotational Sensor to Decipher Volcano Seismic Signals on Etna, Italy. *Journal of Geophysical Research: Solid Earth*. doi: 10.1029/2021jb023617
- Eibl, E. P. S., Thordarson, T., Höskuldsson, Á., Gudnason, E. Á., Dietrich, T., Hersir, G. P., & Ágústsdóttir, T. (2023). Evolving shallow conduit revealed by tremor and vent activity observations during episodic lava fountaining of the 2021 Geldingadalir eruption, Iceland. *Bulletin of Volcanology*, 85(2). doi: 10.1007/s00445-022-01622-z
- Falsaperla, S., Alparone, S., D’Amico, S., Grazia, G., Ferrari, F., Langer, H., ... Spampinato, S. (2005, nov). Volcanic tremor at Mt. Etna, Italy, preceding and accompanying the eruption of July - August, 2001. *Pure and Applied Geophysics*, 162(11), 2111–2132. doi: 10.1007/s00024-005-2710-y
- Fehler, M. (1983). Observations of volcanic tremor at Mount St. Helens. *Journal of Geophysical Research*, 88(B4), 3476–3484.
- Fischer, T., Hrubcová, P., Salama, A., Doubravová, J., Horálek, J., Ágústsdóttir, T., ... Hersir, G. P. (2022). Swarm seismicity illuminates stress transfer prior to the 2021 Fagradalsfjall eruption in Iceland. *Earth and Planetary Science Letters*.
- Flóvenz, Ó. G., Wang, R., Hersir, G. P., Dahm, T., Hainzl, S., Vassileva, M., ... Milkereit, C. (2022). Cyclical geothermal unrest as a precursor to Iceland’s 2021 Fagradalsfjall eruption. *Nature Geoscience*, 15, 397–404. doi: 10.21203/rs.3.rs-636186/v1
- Geirsson, H., Parks, M., Sigmundsson, F., Ófeigsson, B. G., Drouin, V., Ducrocq, C., ... Hooper, A. (2022). Co-eruptive subsidence during the 2021 Fagradalsfjall eruption: geodetic constraints on magma source depths and stress changes. In *Egu general assembly 2022, vienna, austria, 23–27 may 2022, egu22-12435*. doi: 10.5194/egusphere-egu22-12435
- Geirsson, H., Parks, M., Vogfjörð, K., Einarsson, P., Sigmundsson, F., Jónsdóttir, K., ... Ducrocq, C. (2021). The 2020 volcano-tectonic unrest at Reykjanes Peninsula, Iceland: stress triggering and reactivation of several volcanic systems. In *Egu general assembly conference abstracts*. doi: 2021EGUGA..23.7534G
- Greenfield, T., Winder, T., Rawlinson, N., MacLennan, J., White, R. S., Ágústsdót-



- 849 tir, T., ... Horálek, J. (2022). Deep long period seismicity preceding and  
 850 during the 2021 Fagradalsfjall eruption, Iceland. *Bulletin of Volcanology*,  
 851 84(12). Retrieved from <https://doi.org/10.1007/s00445-022-01603-2>  
 852 doi: 10.1007/s00445-022-01603-2
- 853 Halldórsson, S. A., Marshall, E. W., Caracciolo, A., Matthews, S., Bali, E., Ras-  
 854 mussen, M. B., ... Stefánsson, A. (2022). Rapid source shifting of a deep  
 855 magmatic system revealed by the Fagradalsfjall eruption, Iceland. *Nature*.
- 856 Heimann, S., Kriegerowski, M., Isken, M., Cesca, S., Daout, S., Grigoli, F., ...  
 857 Dahm, T. (2017). *Pyrocko - An open-source seismology toolbox and library. V.*  
 858 *0.3* (Tech. Rep.). GFZ. doi: 10.5880/GFZ.2.1.2017.001
- 859 Heliker, C., & Mattox, T. N. (2003). The first two decades of the Pu'u 'Ō'ō-  
 860 Kūpaianaha eruption: Chronology and selected bibliography. *U.S. Geological*  
 861 *Survey Professional Paper*.
- 862 Jónsson, J. (1983). Eldgos á sögulegum tíma á Reykjanesi (in Icelandic). *Nát-  
 863 túrufræðingurinn*, 52, 127–174.
- 864 Journeau, C., Shapiro, N. M., Seydoux, L., Soubestre, J., Koulakov, I. Y., Jakovlev,  
 865 A. V., ... Jaupart, C. (2022). Seismic tremor reveals active trans-crustal mag-  
 866 matic system beneath Kamchatka volcanoes. *Science Advances*, 8(5), 1–10.  
 867 doi: 10.1126/sciadv.abj1571
- 868 Keiding, M., Lund, B., & Árnadóttir, T. (2009). Earthquakes, stress, and strain  
 869 along an obliquely divergent plate boundary: Reykjanes Peninsula, southwest  
 870 Iceland. *Journal of Geophysical Research: Solid Earth*, 114(9), 1–16. doi:  
 871 10.1029/2008JB006253
- 872 Konstantinou, K. I., & Schlindwein, V. (2003). Nature, wavefield proper-  
 873 ties and source mechanism of volcanic tremor: A review. *Journal of Vol-  
 874 canology and Geothermal Research*, 119(1-4), 161–187. doi: 10.1016/  
 875 S0377-0273(02)00311-6
- 876 Koyanagi, R. Y., Chouet, B. A., & Aki, K. (1987). Origin of volcanic tremor in  
 877 Hawaii, part I. Data from the Hawaiian Volcano Observatory, 1969-1985. In  
 878 R. W. Decker, T. W. Wright, & P. H. Stauffer (Eds.), *U.s. geological survey*  
 879 *professional paper 1350* (Vol. v. 2, pp. p. 1221–1257). U.S. Geol. Surv. Prof.  
 880 Pap., 1350.
- 881 Lamb, O. D., Gestrinch, J. E., Barnie, T. D., Jónsdóttir, K., Ducrocq, C., Shore,  
 882 M. J., ... Lee, S. J. (2022). Acoustic observations of lava fountain activity  
 883 during the 2021 Fagradalsfjall eruption , Iceland 1 Introduction. *Bulletin of*  
 884 *Volcanology*, 84(96). doi: 10.1007/s00445-022-01602-3
- 885 Langer, H., Falsaperla, S., Masotti, M., Campanini, R., Spampinato, S., & Messina,  
 886 A. (2009). Synopsis of supervised and unsupervised pattern classification tech-  
 887 niques applied to volcanic tremor data at Mt Etna, Italy. *Geophysical Journal*  
 888 *International*, 178(2), 1132–1144. doi: 10.1111/j.1365-246X.2009.04179.x
- 889 Li, K. L., Bean, C. J., Bell, A. F., Ruiz, M., Hernandez, S., & Grannell, J. (2022).  
 890 Seismic tremor reveals slow fracture propagation prior to the 2018 eruption at  
 891 Sierra Negra volcano, Galápagos. *Earth and Planetary Science Letters*, 586,  
 892 117533. Retrieved from <https://doi.org/10.1016/j.epsl.2022.117533>  
 893 doi: 10.1016/j.epsl.2022.117533
- 894 McNutt, S. R. (1987). Volcanic tremor at Pavlof Volcano, Alaska, October 1973-  
 895 April 1986. *Pure and Applied Geophysics PAGEOPH*, 125(6), 1051–1077. doi:  
 896 10.1007/BF00879368
- 897 McNutt, S. R. (1996). Seismic Monitoring and Eruption Forecasting of Volcanoes:  
 898 A review of the State-of-the-Art and Case Histories. In R. Scarpa & Tilling  
 899 (Eds.), *Monitoring and mitigation of volcano hazards*. Springer-Verlag Berlin  
 900 Heidelberg. doi: 10.1007/978-3-642-80087-0
- 901 McNutt, S. R., & Nishimura, T. (2008, nov). Volcanic tremor during eruptions:  
 902 Temporal characteristics, scaling and constraints on conduit size and pro-  
 903 cesses. *Journal of Volcanology and Geothermal Research*, 178(1), 10–18. doi:

- 10.1016/j.jvolgeores.2008.03.010
- McNutt, S. R., Thompson, G., Johnson, J., Angelis, S. D., & Fee, D. (2015). *Seismic and Infrasonic Monitoring* (Second Edi ed.). Elsevier Inc. Retrieved from <http://dx.doi.org/10.1016/B978-0-12-385938-9.00063-8> doi: 10.1016/B978-0-12-385938-9.00063-8
- Michon, L., Staudacher, T., Ferrazzini, V., Bachélery, P., & Marti, J. (2007, nov). April 2007 collapse of Piton de la Fournaise: A new example of caldera formation. *Geophysical Research Letters*, 34(21). doi: 10.1029/2007GL031248
- Moschella, S., Cannata, A., Di Grazia, G., & Gresta, S. (2018). Insights into lava fountain eruptions at mt. Etna by improved source location of the volcanic tremor. *Annals of Geophysics*, 61(4). doi: 10.4401/ag-7552
- Patane, D., Di Grazia, G., Cannata, A., Montalto, P., & Boschi, E. (2008). Shallow magma pathway geometry at Mt. Etna volcano. *Geochemistry, Geophysics, Geosystems*, 9(12). doi: 10.1029/2008GC002131
- Patrick, M. R., Orr, T., Wilson, D., Dow, D., & Freeman, R. (2011). Cyclic spattering, seismic tremor, and surface fluctuation within a perched lava channel, Kīlauea Volcano. *Bulletin of Volcanology*, 73(6), 639–653. doi: 10.1007/s00445-010-0431-2
- Pedersen, G. B. M., Belart, J. M. C., Óskarsson, B. V., Gudmundsson, M. T., Gies, N., Högnadóttir, T., ... Oddsson, B. (2022). Volume, effusion rate, and lava transport during the 2021 Fagradalsfjall eruption: Results from near real-time photogrammetric monitoring. *Geophysical Research Letters*. Retrieved from <https://doi.org/10.1002/essoar.10509177.1> doi: 10.1029/2021GL097125
- Privitera, E., Sgroi, T., & Gresta, S. (2003). Statistical analysis of intermittent volcanic tremor associated with the September 1989 summit explosive eruptions at Mount Etna, Sicily. *Journal of Volcanology and Geothermal Research*, 120, 235–247. Retrieved from [www.elsevier.com/locate/jvolgeores](http://www.elsevier.com/locate/jvolgeores)
- Romero, J. E., Burton, M., Cáceres, F., Taddeucci, J., Civico, R., Ricci, T., ... Perez, N. M. (2022). The initial phase of the 2021 Cumbre Vieja ridge eruption (Canary Islands): Products and dynamics controlling edifice growth and collapse. *Journal of Volcanology and Geothermal Research*, 431(August). doi: 10.1016/j.jvolgeores.2022.107642
- Sæmundsson, K., & Sigurgeirsson, M. Á. (2013). The Reykjanes Peninsula. In J. Sólves, F. Sigmundsson, & B. Bessason (Eds.), *Natural hazards in iceland, volcanic eruptions and earthquakes (in icelandic)*. (pp. 379–401). Reykjavík: Viðlagatrygging Íslands/Háskólaútgáfan.
- Sæmundsson, K., Sigurgeirsson, M. Á., & Friðleifsson, G. Ó. (2020). Geology and structure of the Reykjanes volcanic system, Iceland. *Journal of Volcanology and Geothermal Research*, 391, 106501. Retrieved from <https://www.sciencedirect.com/science/article/pii/S0377027317305474> doi: <https://doi.org/10.1016/j.jvolgeores.2018.11.022>
- Scott, S. W., & Al., E. (2023). Near-surface magma flow instability drives cyclic lava fountaining at Fagradalsfjall, Iceland. *Bull. Volcanol.*
- Sigmundsson, F., Einarsson, P., Hjartardóttir, Á. R., Drouin, V., Jónsdóttir, K., Árnadóttir, T., ... Ófeigsson, B. G. (2020). Geodynamics of Iceland and the signatures of plate spreading. *Journal of Volcanology and Geothermal Research*, 391, pagerange. Retrieved from <https://doi.org/10.1016/j.jvolgeores.2018.08.014> doi: 10.1016/j.jvolgeores.2018.08.014
- Sigmundsson, F., Parks, M., Hooper, A., Geirsson, H., Vogfjörð, K. S., Drouin, V., ... Ágústsdóttir, T. (2022). Deformation and seismicity decline before the 2021 Fagradalsfjall eruption. *Nature*, 609(7927), 523–528. doi: 10.1038/s41586-022-05083-4
- Sigurgeirsson, M. Á. (1995). The Younger-Stampar eruption at Reykjanes, SW-Iceland. *Náttúrufræðingurinn*, 64, 211–230.

- 959 Spampinato, L., Sciotto, M., Cannata, A., Cannavó, F., La Spina, A., Palano, M.,  
 960 ... Caltabiano, T. (2015, jun). Multiparametric study of the February-April  
 961 2013 paroxysmal phase of Mt. Etna New South-East Crater. *Geochemistry,*  
 962 *Geophysics, Geosystems*, 16(6), 1932–1949. doi: 10.1002/2015GC005795
- 963 Staudacher, T., Ferrazzini, V., Peltier, A., Kowalski, P., Boissier, P., Catherine, P.,  
 964 ... Massin, F. (2009, jul). The April 2007 eruption and the Dolomieu crater  
 965 collapse, two major events at Piton de la Fournaise (La Réunion Island, In-  
 966 dian Ocean). *Journal of Volcanology and Geothermal Research*, 184(1-2),  
 967 126–137. Retrieved from [http://linkinghub.elsevier.com/retrieve/pii/](http://linkinghub.elsevier.com/retrieve/pii/S0377027308005945)  
 968 [S0377027308005945](http://linkinghub.elsevier.com/retrieve/pii/S0377027308005945) doi: 10.1016/j.jvolgeores.2008.11.005
- 969 Thompson, G., McNutt, S. R., & Tytgat, G. (2002, dec). Three distinct  
 970 regimes of volcanic tremor associated with the eruption of Shishaldin  
 971 Volcano, Alaska 1999. *Bulletin of Volcanology*, 64(8), 535–547. doi:  
 972 10.1007/s00445-002-0228-z
- 973 Thordarson, T., Bindeman, I. N., Deegan, F., Troll, V. R., Höskuldsson, A., More-  
 974 land, W. M., ... Stroganova, L. (2023). Diverse mantle components with  
 975 invariant oxygen isotopes: the 2021-ongoing Fagradalsfjall Fires, Iceland. In  
 976 *Iavcei*.
- 977 Trnkoczy, A. (2012). Understanding and parameter setting of STA/LTA trigger algo-  
 978 rithm. *New manual of seismological observatory practice 2*, 1–41. doi: 10.2312/  
 979 GFZ.NMSOP-2\_IS\_8.11
- 980 Viccaro, M., Garozzo, I., Cannata, A., Di Grazia, G., & Gresta, S. (2014). Gas  
 981 burst vs. gas-rich magma recharge: A multidisciplinary study to reveal fac-  
 982 tors controlling triggering of the recent paroxysmal eruptions at Mt. Etna.  
 983 *Journal of Volcanology and Geothermal Research*, 278-279, 1–13. doi:  
 984 10.1016/j.jvolgeores.2014.04.001
- 985 Yukutake, Y., Honda, R., Harada, M., Doke, R., Saito, T., Ueno, T., ... Morita,  
 986 Y. (2017). Analyzing the continuous volcanic tremors detected during the  
 987 2015 phreatic eruption of the Hakone volcano. *Earth, Planets and Space*,  
 988 69(1). Retrieved from <https://doi.org/10.1186/s40623-017-0751-y> doi:  
 989 10.1186/s40623-017-0751-y